Supporting Information

Metabolic traits of *Ca.* Accumulibacter clade IIF strain SCELSE-1 using amino acids as carbon sources for enhanced biological phosphorus removal

Guanglei Qiu[1,6*], Xianghui Liu[1], Nay Min Min Thaw Saw[1], Yingyu Law[1], Rogelio Zuniga-Montanez[1,2], Sara Swa Thi[1], Thi Quynh Ngoc Nguyen[1], Per H. Nielsen[1,3], Rohan B.H. Williams[4], Stefan Wuertz[1,2,5*]

[1]*Singapore Centre for Environmental Life Sciences Engineering, Nanyang Technological University, Singapore 637551, Singapore.*

[2]*Department of Civil and Environmental Engineering, One Shields Avenue, University of California, Davis, California 95616, USA.*

[3]*Centre for Microbial Communities, Department of Chemistry and Bioscience, Aalborg University, DK-9220, Aalborg, Denmark.*

[4]*Singapore Centre for Environmental Life Sciences Engineering, National University of Singapore, Singapore 119077, Singapore.*

[5]*School of Civil and Environmental Engineering, Nanyang Technological University, Singapore 639798, Singapore*

[6]*School of Environment and Energy, South China University of Technology, Guangzhou 510006, China*

Corresponding Author: swuertz@ntu.edu.sg (S.W.); qiugl@scut.edu.cn (G.Q.)

Supporting Information: 57 pages, 6 tables, 13 figures

S1. Material and Methods

S1.1 EBPR reactor operation.

A sequencing batch reactor (SBR) with a working volume of 5.4 L was inoculated with sludge from an EBPR enrichment reactor. A slow feeding strategy was applied for the reactor operation, which has been shown to benefit the proliferation of *Ca.* Accumulibacter. The SBR was operated with 6-h cycles, including a 60-min feed, a 20-min anaerobic, a 180-min aerobic, and a 100-min settling/decant stage. In each cycle, 2.35 L of synthetic wastewater composed of 0.53 L of solution A (containing 1.02 g/L NH_4Cl, 1.2 g/L $MgSO_4 \cdot 7\ H_2O$, 0.01g/L peptone, 0.01g/L yeast extract and 6.8 g/L sodium acetate) and 1.82 L of solution B (0. 312 g/L $K_2HPO_4 \cdot 3\ H_2O$, 0.185 g/L KH_2PO_4, 0.75 mg/L $FeCl_3 \cdot 6\ H_2O$, 0.015 mg/L $CuSO_4 \cdot 5H_2O$, 0.03 mg/L $MnCl_2$, 0.06 mg/L $ZnSO_4$, 0.075 mg/L $CoCl_2$, 0.075 mg/L H_3BO_3, 0.09 mg/L KI and 0.06 mg/L $Na_2MoO_4 \cdot 2\ H_2O$) were introduced into the reactor. The reactor was operated at 30^{o}C with an HRT and SRT of 12 h and 11 d, respectively. The pH was controlled at 7.00 - 7.60, with DO levels maintained at 0.8-1.2 mg/L during the aerobic phase.

S1.2 Amino acid uptake mechanism.

To study the uptake mechanisms with acetate, glutamate and aspartate as carbon sources, fresh activated sludge collected at the end of the aerobic stage was diluted to a MLSS concentration of 0.5 g/L. Two hundred millilitres of mixed liquor were added to nine batch reactors. Three reactors were supplied with carbonyl cyanide m-chlorophenylhydrazone (CCCP, final concentration of 100 mM), and three with N-N'-dicyclohexylcarboiimide (DCCD; final concentration of 50 mM). CCCP is an uncoupler that inhibits the build-up of the electro-chemical potential (i.e. proton motive force, PMF) across the cell membrane. DCCD is an F1-F0 ATPase inhibitor capable of significantly reducing the intracellular ATP levels via covalent modification of membrane-bound ATPase.[16,17] The sludge was incubated under anaerobic conditions for 30 min at 30 ^{o}C and a pH of 7.0 for the inhibitory effects to take place. Three reactors with no inhibitor added served as controls. After incubation, acetate,

aspartate or glutamate were added to each set of reactors at a final concentration of 8.33 mmol C/L (TOC content of 100 mg/L). Water and biomass samples were collected at time intervals for TOC and PO_4^{3-}-P analysis.

S1.3 DNA extraction, 16S rRNA gene amplicon sequencing and metagenomic analysis

For the microbial community analysis, 2 ml of mixed liquor were collected on Day 152 and Day 166 from the end of the aerobic stage and stored at -80°C before DNA extraction. Genomic DNA was extracted using the Fast DNATM 2 mL SPIN Kit for Soil samples (MP Biomedicals, CA, USA), following the optimised protocol for activated sludge.[1] Bacterial 16S rRNA gene amplicon sequencing was performed, targeting the V1-V3 region (primer set: 27F AGAGTTTGATCCTGGCTCAG and 534R ATTACCGCGGCTGCTGG). PCR amplification was carried out in a 25-µl PCR matrix containing 10 ng of genomic DNA, 400 nM dNTPs, 1.5 mM $MgSO_4$, 2 mU Platinum R Taq DNA polymerase high fidelity, 1× Platinum R High Fidelity buffer (Thermo Fisher Scientific, MA, USA) and a pair of barcoded library adaptors (400 nM), with a thermo cycler setting of initial denaturation at 95°C for 2 min, 30 cycles of 95°C for 20 s, 56°C for 30 s, 72°C for 60 s, and final elongation at 72°C for 5 min. All PCR reactions were run in duplicate and pooled afterwards. The amplicon libraries were purified using the Agencourt R AMpure XP bead protocol (Beckmann Coulter, CA, USA) with 1.8 bead solution/PCR solution ratio. Based on library concentrations and calculated amplicon sizes, the samples were pooled in equimolar concentrations. The library pool was sequenced on a MiSeq (Illumina, CA, US) using a MiSeq Reagent kit v3 (2×300 paired end). Pre-processing of all amplicon libraries was performed according to Albertsen et al.[1] Taxonomy was assigned using MiDAS v.1.20.[2]

For metagenomic DNA, two samples were collected at Day 146 and Day 152. Sequencing library preparation was performed using a modified version of the Illumina TruSeq DNA Sample Preparation protocol: For the sample, 1 µg of the DNA was sheared on a Covaris S220 to approximately 300 bp, following the manufacturer's recommendation. Size selection was performed on a Sage Science Pippin Prep instrument, using a 2% EtBr agarose cassette and selecting for a tight peak around 400 bp. Each library was tagged with a TruSeq LT DNA barcode (Illumina) to allow for library pooling prior to sequencing. Library quantitation was performed using the Picogreen assay (Invitrogen) and the average library size was determined by running the libraries on a Bioanalyzer DNA 7500 chip (Agilent). Library concentrations were normalized to 4 nM and validated by qPCR on a ViiA-7 real-time thermocycler (Applied Biosystems), using qPCR primers recommended by Illumina in their qPCR protocol, and the Illumina PhiX control library was used as a standard. Libraries were then

combined in one pool, which was sequenced across two lanes of an Illumina HiSeq2500 sequencing run at a read-length of 150 bp paired-end. Raw reads have been submitted to NCBI and are accessible under the BioProject PRJNA532338.

Sequencing of these samples generated 31.4 and 31 Gb of data for the samples on Day146 and Day152, respectively. Illumina reads were processed to cut the adaptor and quality-trimmed using Trimmomatic version 0.36 [3]. Paired end reads from sample Day 152 were then merged using IDBA version 1.1.1 fq2fa and assembled into contigs using idba_ud [4]. Reads from Day 146 and Day 152 were then mapped to those contigs using Bowtie2 version 2.3.4.3 [5] and sam files were converted into bam files and then sorted and indexed using samtools [6]. Coverages file are generated using CONCOCT version 1.0.0 script gen_input_table.py [7]. Assembled contigs larger than 1500bp were then binned using CONCOCT. Bin information is summarized in Table S1. In total 128 bins were found. Completeness, redundancy and strain heterogeneity were assessed using CheckM v1.0.7 [8].

There was one bin (bin0) with a high completeness (95.24%) and low contamination rate (0.6%), and it was annotated to the marker set lineage UID3971. This is a possible *Ca.* Accumulibacter bin. The average coverages for bin0 are around 375 and 408 for Day 146 and Day 152. Mash [9] was used to check the taxonomic information for bin0. The genome of this bin was uploaded into PATRIC [10] (https://www.patricbrc.org). The Similar Genome Finder Service in PATRIC (https://www.patricbrc.org/app/GenomeDistance) was used to find similar public genomes in PATRIC. The genome distance estimation was compute using Mash/MinHash. The top 10 similar genomes of bin0 are listed in Table S2. The result suggested that bin0 is an *Ca.* Accumulibacter bin with the closest relationship with *Ca.* Accumulibacter sp. BA-94. The average nucleotide identity(ANI) [11] among bin0 and published *Ca.* Accumulibacter genomes was determined according to the method described by Richter and Rosselló-Móra [12] as implemented in the python script 'CALCULATE_ANI.PY' (https://github.com/ctSkennerton/scriptShed/blob/master/calculate_ani.py). Results showed that bin0 shared ANI values of 84.7-90.8% with other *Ca.* Accumulibacter genomes (Figure S1), suggesting that bin0 represents a new species of *Ca.* Accumulibacter (based on the typical percentage threshold for species boundary of 95% ANI).

bin0 was further checked with Quast [13] and annotated with Prokka v1.12 [14], finding that this bin contained 253 contigs (the length ranged from 1,657 to 100,190 bp with a mean of 17,616 bp) and had a total sequence length of 4.25Mb, with an average GC content of 66.1%. The draft genome sequence encodes 4,062 genes together with 38 tRNAs genes (Table S3).

To further identify the taxonomic information of bin0, we looked for 16S rRNA and *ppk1* genes in this genome. One *ppk1* gene was found in the bin. But there was no 16S rRNA gene. From the 16S amplicon sequencing data and CONCOC binning result, there was likely only one strain of *Ca.* Accumulibacter in this community. To recover the full length 16S rRNA gene, EMIRGE [15] was used. An almost full-length 16S rRNA gene (1,407 bp) was constructed and SILVA Incremental Aligner (SINA) [16] suggests it to be *Ca.* Accumulibacter with 99.6% sequence identity.

The *ppk1* gene has been used to partition the *Ca.* Accumulibacter lineage. A *ppk1* (2,121 bp) homologue identified in a long contig (contig-100_2131, 17,267 bp). A phylogenetic tree constructed from this *ppk1* gene with other representative *ppk1* genes of *Ca.* Accumulibacter genomes and clone sequences available at NCBI were used to classify into 1 of the 14 clades described to date [17,18]. According to the phylogenetic tree topology of the *ppk1* gene (Figure S2), *ppk1* of bin0 clustered with sequences previously classified as clade IIF. It shares a 95.13% nucleotide identity with BPBW3662 (GenBank EU433148). The most similar genome *ppk1* gene is from *Ca.* Accumulibacter sp. BA-94 (on contig JEMZ01000181.1) and the encoding protein is EXI82049.1.

Genome-based phylogeny analysis based on a concatenated alignment of 92 maker genes of the draft genome recovered in this work and the *Ca.* Accumulibacter draft genomes published in GeneBank using UBCG pipeline [19] further confirmed that the draft genome represents a new species (Figure S3).

Collectively, these results suggest that a draft genome of a new species of *Ca.* Accumulibacter was recovered. This strain is thus named "*Candidatus* Accumulibacter clade IIF strain SCELSE-1". This Whole Genome Shotgun project has been deposited at DDBJ/ENA/GenBank under the accession SZXR00000000. The version described in this paper is version SZXR01000000.

S1.4 Fluorescence in situ hybridisation (FISH)

Activated sludge collected at the end of the aerobic stage was immediately fixed using 4% paraformaldehyde (final concentration) at 4°C for 2-3 h. The fixed activated sludge samples were washed with 1× phosphate-buffered saline (PBS) solution. Washed samples were stored at -20°C in a mixed solution of 1×PBS and 100% ethanol (50:50) before FISH analysis. Organisms of interest were detected using EUB probe mix, targeting most Bacteria (EUB338, EUB338II and EUB338III)[20], and PAOmix (PAO651, PAO462 and PAO846)[21] and GAOmix (GAO431 and GAO989)[22] targeting *Ca.* Accumulibacter and *Ca*. Competibacter, respectively. FISH images were obtained using a Zeiss LSM780 confocal microscope system (Carl Zeiss, Germany). The biovolume was measured using Image pro plus 6.0 (Media Cybernetics, U.S.)

S1.5 NMR analysis

Mixed liquor samples were collected at the beginning of the experiment, and at the end of anaerobic and aerobic phases in the anaerobic-aerobic full-cycle study. The samples were centrifuged immediately at 12,000 rpm for 2 min at 4^{o}C. The supernatant was discarded and the pellet was snap-frozen in liquid nitrogen and freeze-dried. The lyophilized samples were stored at -80^{o}C prior to the extraction of the intracellular storage compounds. Twenty-five milligrams of sludge powders from each freeze-dried sample were extracted using 2 mL of 50% (v/v) methanol. After vortexing for 1 min and sonicating for 10 min, the samples were put in a rotary shaker for 30 min at room temperature. After centrifugation at 12,000 rpm for 5 min, the supernatants were collected, and the pellets were re-extracted with 1 ml of 50% (v/v) methanol. Supernatants were combined and dried by using vacuum evaporator. The dried samples were re-constituted in 0.5 ml of 4.8 mM 2,2,3,3-tetradeutero-3-(trimethylsilyl) propionate in D_2O and loaded in 5-mm NMR tubes. ^{1}H-NMR analysis was performed on a 600 MHz Bruker In Vitro Diagnostics Research (IVDr) system comprises of an AVANCE III HD console, a ascend 600 magnet and a 5-mm broadband inverse probe, operating at 600.13 MHz. Analysis of the NMR spectra was performed using TopSpin V3.6.0 (Bruker, Billerica, MA, USA).

S1.6 Pathways, ATP, reducing power and PMF balance in anaerobic acetate, aspartate and glutamate metabolisms of *Ca.* Accumulibacter

S1.6.1 Acetate as a carbon source

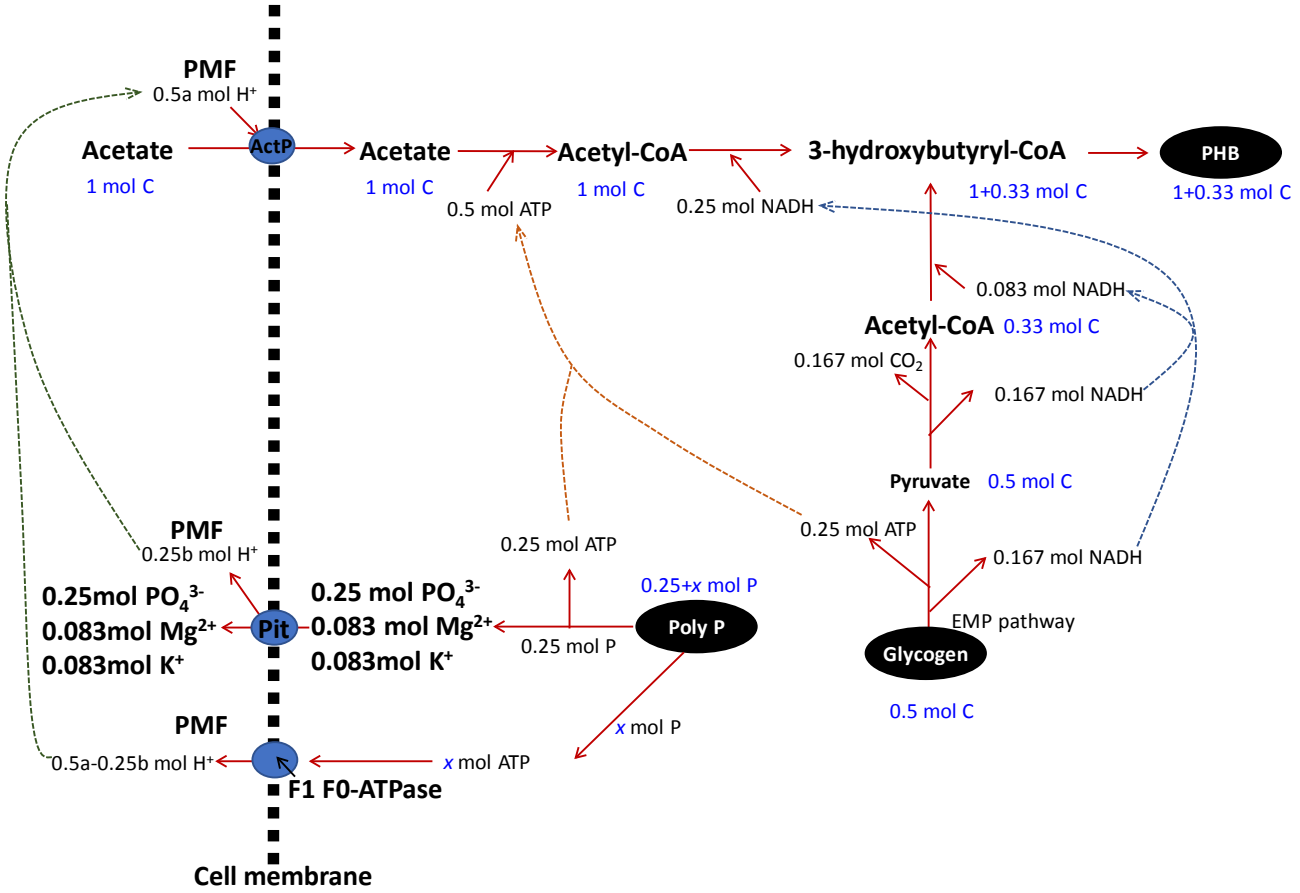

Figure S1.6.1 Metabolic pathways, ATP, reducing power and PMF balance of *Ca.* Accumulibacter with acetate as carbon source.

The activation of 1 mol C as acetate (into acetyl-CoA) requires 0.5 mol ATP and the subsequent reduction of 1 mol C as acetyl-CoA (to 3-hydroxybutyryl-CoA) to form PHB needs 0.25 mol NADH [23] (Figure S1.6.1).

Glycolysis of 1 mol C as glycogen and its subsequent transformation to 0.67 mol C as PHB generates 0.5 mol ATP and 0.5 mol NADH [23] (Figure S1.6.1).

To balance the NADH, 0.5 mol C as glycogen is required for the transformation of 1 mol C as acetate. The glycolysis of 0.5 mol C as glycogen, in the meantime, generates 0.25 mol ATP. This ATP is used

for the activation of acetate (Figure S1.6.1). To balance the ATP, an additional 0.25 mol ATP is needed (for the activation of 1 mol C as acetate). These 0.25 mol ATP are generated from poly-P hydrolysis. The hydrolysis of 1 mol P as poly-P generates 1 mol ATP (Figure S1.6.1). Thus, 0.25 mol P as poly-P is required (Figure S1.6.1). The hydrolysis of 0.25 mol P as poly-P (and the subsequent consumption of the ATP produced from poly-P hydrolysis) generates 0.25 mol PO_4^{3-}, 0.083 mol Mg^{2+} and 0.083 mol K^+. The efflux of H^+ in symport with these ions through the inorganic phosphate transporter (Pit) generates PMF.[24,25] Assume that efflux of 1 mol of PO_4^{3-} results in the translocation of b mol H^+. Based on the charge balance (i.e., a net flux of negative charge out of the cell), b<2 (1 mol of PO_4^{3-} carries 3 mol negative charges. 0.33 mol Mg^{2+} and 0.33 mol K^+ carry 1 mol positive charges in total. Thus, the amount of H^+ translocated with the efflux of 1 mol of PO_4^{3-} is no more than 2 mol). 0.25 mol of ATP would result in the translocation of 0.25b mol H^+.

Assume that the transport of 1 mol (2 mol C) acetate is achieved in symport with 1 mol H^+ through ActP, having a net flux of positive charge into the cell, i.e. a >1.

Since b<2 and a>1, then 0.25b (generated)<0.5a (required for the uptake of 1 mol C as acetate). It is clear that the PMF generated via efflux of H^+ in symport with PO_4^{3-} is insufficient for the uptake of acetate, i.e., pathways to generate additional PMF (0.5a-0.25b mol H^+) are needed.

The DCCD inhibition experiment suggested that around 25% of PMF was generated via the reverse operation of F1-F0 ATPase, i.e., 0.5a-0.25b≈0.125a, b≈1.5a (a>1; b<2).

S1.6.2 Aspartate as a carbon source

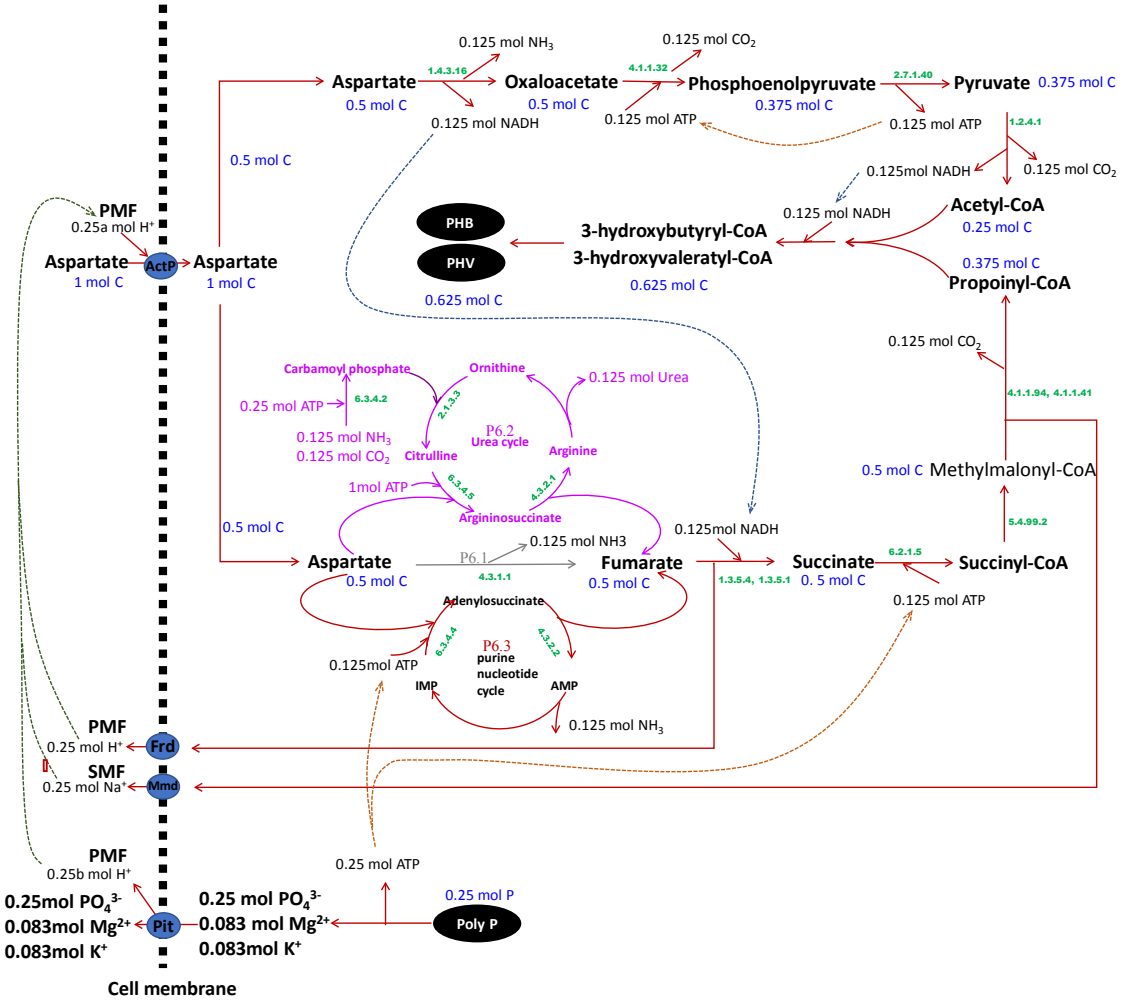

Figure S1.6.2 Metabolic pathways, ATP, reducing power and PMF balance of *Ca.* Accumulibacter with aspartate as carbon source.

0.5 mol C as aspartate undergoes oxidative deamination catalyzed by L-aspartate oxidase [EC: 1.4.3.16] generates 0.5 mol C as oxaloacetate (and 0.125 mol NH_3). L-aspartate oxidase can use both O_2 and fumarate in cofactor re-oxidation, which enables it to function under both aerobic and anaerobic conditions.[26] 0.5 mol C as oxaloacetate is converted into 0.375 mol C as phosphoenolpyruvate (catalyzed by phosphoenolpyruvate carboxykinase [EC: 4.1.1.32] at the expense of 0.125 mol ATP) and then to 0.375 mol C as pyruvate (catalyzed by pyruvate kinase [EC: 2.7.1.40] and results in the generation of 0.125 mol ATP). 0.375 mol C as pyruvate is then converted [EC: 1.2.4.1] into 0.25 mol C as acetyl-CoA following the traditional acetate metabolic pathway and results in the production of 0.125 mol NADH.

The anaerobic operation of L-aspartate oxidase [EC: 1.4.3.16] needs fumarate as an electron acceptor. Fumarate can be readily generated from aspartate. *Ca.* Accumulibacter clade IIF strain SCELSE-1

(and also the clade IIA strain UW-1) encode three pathways for the conversion of aspartate to fumarate: (P6.1, Figure S1.6.2) direct conversion through the activity of aspartate ammonia-lyase [EC: 4.3.1.1]; (P6.2, Figure S1.6.2) formation via the purine nucleotide cycle (EC: 6.3.4.4; EC: 4.3.2.2) at the expense of 0.125 mol ATP (per 0.5 mol C of fumarate production); or (P6.3, Figure S1.6.2) generation via the urea cycle (EC: 6.3.4.5; EC: 4.3.2.1), which consumes more ATP (0.375 mol per 0.5 mol C of fumarate produced), but can condense the NH_3 (0.125 mol) cleaved from the aspartate together with 0.125 mol of free NH_3 to 0.125 mol of urea. Compared to the direct conversion (P6.1), the purine nucleotide cycle (P6.3) could provide a higher production rate of fumarate to meet the cofactor demand of L-aspartate oxidase to convert aspartate to oxaloacetate.[27] The urea cycle (P6.2) consumes more ATP, but could effectively decrease the in-cell NH_3 content, thus avoiding inhibition from free NH_3.[28] The subsequent transformation of 0.5 mol C as fumarate (mediated by fumarate reductase EC: 1.3.5.4 and EC: 1.3.5.1) into 0.5 mol C as succinate balances the oxidative strength generated during oxidative deamination of aspartate and results in the translocation of 0.25 mol H^+. 0.5 mol C as succinate is then activated (EC: 6.2.1.5) into 0.5 mol C as succinyl-CoA and consumes 0.125 mol ATP, followed by its isomerization (mediated by methylmalonyl-CoA mutase; EC: 5.4.99.2) into methylmalonyl-CoA. The decarboxylation of 0.5 mol C as methylmalonyl-CoA (mediated by methylmalonyl-CoA decarboxylase EC:4.1.1.94 and EC: 4.1.1.41) generates 0.375 mol C as propoinyl-CoA and results in the translocation of 0.25 mol Na^+. [29]

To maintain a redox balance, equal amount of aspartate (i.e. 0.5 mol C each) would be channeled through the above-mentioned two metabolic pathways, which results in (1) the consumption of 0.25 mol ATP (1 mol ATP per mol of fumarate generation via purine nucleotide cycle and 1 mol ATP per mol of succinate activation); (2) the generation of 0.125 mol NADH (pyruvate to acetyl-CoA); (3) the translocation of 0.25 mol H^+ and 0.25 mol Na^+; and (4) the production of 0.25 mol C as acetyl-CoA and 0.375 mol C as propoinyl-CoA (Figure S1.6.2).

The subsequent reduction of 0.25 mol C as acetyl-CoA and 0.375 mol C as propoinyl-CoA into 3-hydroxyvaleratyl-CoA, 3-hydroxy-2-methylvalerate-CoA or 3-hydroxybutyryl-CoA (0.625 mol C in total) consumes 0.125 mol NADH. Given the net production of 0.125 mol NADH in the transformation of pyruvate to acetyl-CoA, no additional NADH would be needed from either glycolysis or the TCA cycle (Figure S1.6.2).

Considering that 0.25 mol ATP (required for fumarate generation via purine nucleotide cycle (P6.3) and succinate activation) is provided by poly-P hydrolysis, a consumption of 0.25 mol P as poly-P is required.

The uptake of aspartate occurs via GltP driven by the PMF. Given that the *p*Ka values of aspartic acid are *p*Ka1 = 1.88, *p*Ka2 = 3.65, and *p*Ka3 = 9.60, the net charge of the aspartate at pH = 7.0 is -1. Assume that the transport of 1 mol (4 mol C) of aspartate is achieved in symport with 1 mol H^+. To maintain a net positive charge transported into the cells, a>1. 0.25a mol H^+ is required for the uptake of 1 mol C as aspartate (Figure S1.6.2).

The hydrolysis of 0.25 mol poly-P (and the subsequent consumption of the 0.25 mol of ATP produced from the hydrolysis of these 0.25 mol of poly-P) generates 0.25 mol PO_4^{3-}, 0.083 mol Mg^{2+} and 0.083 mol K^+; the efflux of H^+ in symport with these ions through Pit (with a net negative charge flowing out of the cell) generates PMF. Assume that efflux of 1 mol of PO_4^{3-} resulted in the translocation of b mol H^+ (as mentioned above, 1 mol of PO_4^{3-} carries 3 mol negative charges and 0.33 mol Mg^{2+} and 0.33 mol K^+ carry 1 mol positive charges in total. Thus, the amount of H^+ translocated with the efflux of 1 mol of PO_4^{3-} is no more than 2 mol, i.e., b<2.) (Figure S1.6.2).

Additionally, the reduction of 0.5 mol C as fumarate to succinate results in the translocation of an additional 0.25 mol H^+ (Figure S1.6.2). In total, 0.25b+0.25 mol H^+ is generated. Assume that the same b≈1.5a is maintained as in the case of acetate, then 0.25b+0.25 (generated) >0.25a (required for the uptake of 1 mol C as aspartate). Clearly, enough PMF is generated from the hydrolysis of poly-P and the fumarate reductase for aspartate uptake. No operation of F1-F0 ATPase is required to generate additional PMF (Figure S1.6.2).

The P/C molar ratio for aspartate uptake in this case is around 0.25. And the aspartate uptake and PHA formation ratio is 0.625 mol C / mol C with an acetyl-CoA and propionyl-CoA molar ratio of 1:1 (Figure S1.6.2).

However, the deamination of aspartate results in the generation of NH_3. *Ca.* Accumulibacter might have to eliminate the toxic effects of the increased intracellular NH_3 concentration by employing the urea cycle at the expense of more ATP.[28] The necessity to activate the urea cycle might depend on the tolerance level of the bacteria, the ability of the bacteria to effectively pump out NH_3 through another pathway, and the extracellular/intracellular pH and NH_3 concentration. In the case where all the fumarate is generated via the urea cycle the P/C molar ratio would increase to 0.5 (3 mol/mol of ATP consumption in the urea cycle compared to 1 mol/mol of ATP consumption in the purine nucleotide cycle for the production of the same amount of 1 mol fumarate). That might explain the higher C/P ratios observed in studies when aspartate was used as a carbon source. [30,31]

S1.6.3 Glutamate as a carbon source

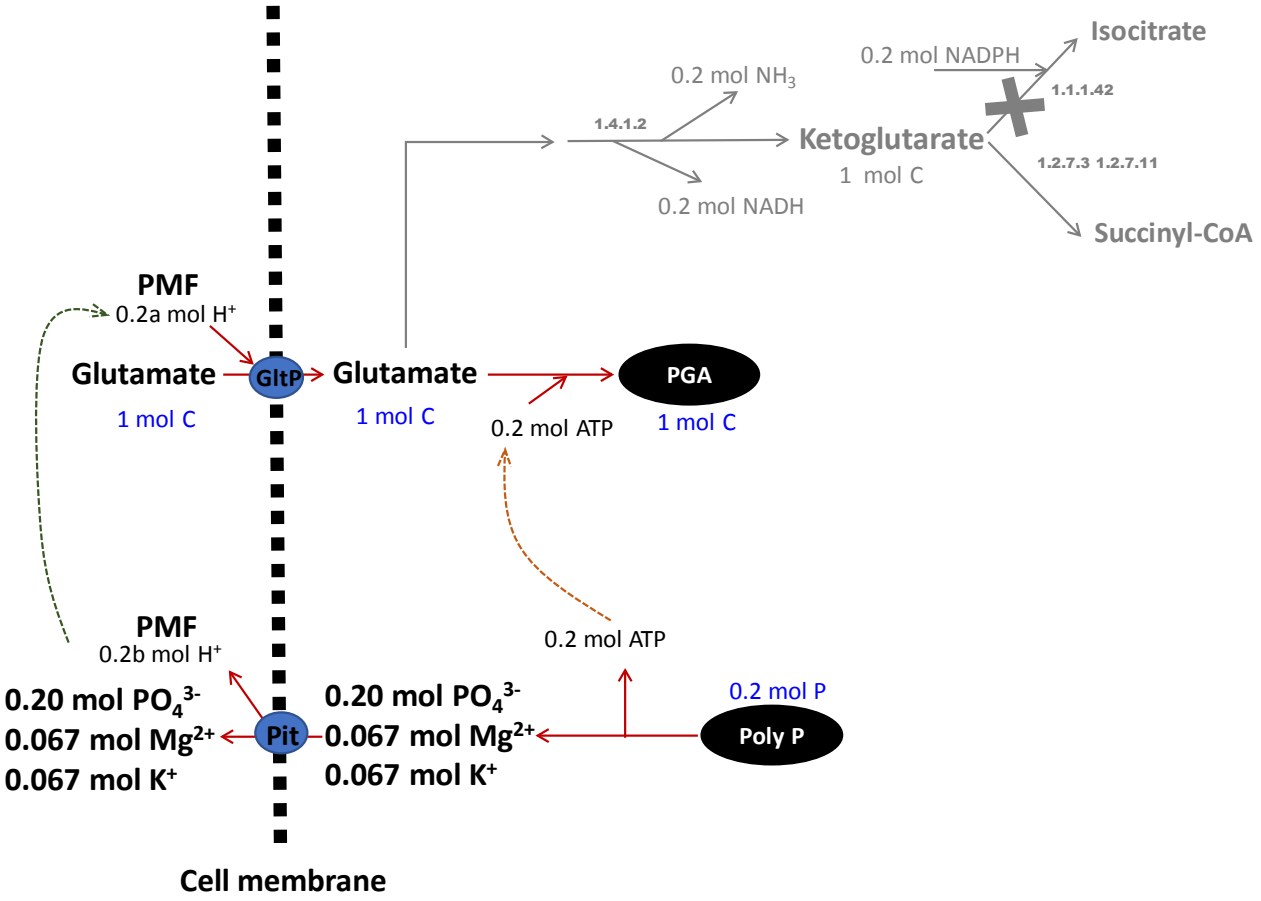

Figure S1.6.3 Metabolic pathways, ATP, reducing power and PMF balance of *Ca.* Accumulibacter with glutamate as carbon source.

Glutamate is taken up via GltP driven by PMF (Figure S1.6.3).

Glutamate can be converted into ketoglutarate with the aid of glutamate dehydrogenase [EC: 1.4.1.2], which results in the generation of NH_3 and NADH. Ketoglutarate could then be channeled to the TCA cycle. However, no significant NH_4^+ release was observed during anaerobic glutamate uptake, suggesting that a majority of glutamate was not converted into ketoglutarate. A possible explanation is that *Ca.* Accumulibacter clade IIF strain SCELSE-1 encodes only an NADP-specific isocitrate dehydrogenase [EC: 1.1.1.42] other than its NAD-specific homologues [EC: 1.1.1.41]. Inside the cells, the ratio of NADP+/NADPH is typically kept low. NADP-specific isocitrate dehydrogenase [EC:1.1.1.42] might use NADH but much more slowly,[30] which creates a barrier for the carboxylation of ketoglutarate to synthesize isocitrate to achieve a reducing power balance (Figure S1.6.3).

Glutamate is assumed to be condensed into poly-glutamate (Figure S1.6.3).

The condensation of 1 mol C as glutamate requires 0.2 mol ATP. This ATP is generated from the hydrolysis (5 mol C) of poly-P (Figure S1.6.3).

Similarly, assume that the hydrolysis of poly-P and the efflux of 1 mol of PO_4^{3-} results in the translocation of b mol H^+ (where $b < 2$, as mentioned above). The condensation of 1 mol C as glutamate requires 0.2 mol P as poly-P and the efflux of 0.2 mol PO_4^{3-} achieves the translocation of 0.2b mol H^+.

The *p*Ka values of glutamic acid are *p*Ka1 = 2.19, *p*Ka2 = 4.25, and *p*Ka3 = 9.67. The net charge of glutamate at pH=7.0 is expected to be -1. Assume that transport of 1 mol glutamate (5 mol C) is achieved in symport with a mol H^+, having a net flux of positive charge into the cell, i.e. $a > 1$. The transport of 1 mol C as glutamate would require 0.2a mol H^+.

Assume that a and b remained at the same ratio as in the case of acetate ($b \approx 1.5a$), thus $0.2b > 0.2a$. Enough PMF is generated for the uptake of glutamate. The result agreed with the finding that no operation of F1-F0 ATPase was required during glutamate uptake (Figure S1.6.3).

Overall, the P/C molar ratio for glutamate uptake is around 0.2.

Table S1: CheckM results of bins from CONCOCT with contig length>=1500.

BinID	Marker	Lineage	Genomes	Markers	Marker sets	0	1	2	3	4	5+	Completeness	Contamination	Strain heterogeneity
81	k__Bacteria	UID203	5449	104	58	0	13	41	32	13	5	100	148.78	1.51
75	root	UID1	5656	56	24	0	0	7	43	6	0	100	206.1	11.05
65	k__Bacteria	UID203	5449	104	58	0	7	95	2	0	0	100	88.24	1.98
24	root	UID1	5656	56	24	0	0	0	12	44	0	100	277.13	1
123	k__Bacteria	UID203	5449	104	58	0	7	94	3	0	0	100	95.16	34.95
17	k__Bacteria	UID2982	88	229	147	1	227	1	0	0	0	99.86	0.68	0
5	k__Bacteria	UID203	5449	104	58	1	38	5	5	17	38	99.14	349.9	6.81
83	c__Alphaproteobacteria	UID3422	26	529	308	36	41	110	178	147	17	98.91	204.35	61.37
101	c__Alphaproteobacteria	UID3422	26	529	308	8	515	6	0	0	0	98.53	1.62	16.67
72	k__Bacteria	UID2570	433	274	183	6	264	3	1	0	0	97.27	2.73	0
114	k__Bacteria	UID1453	901	171	117	10	158	3	0	0	0	96.89	2.14	0
66	k__Bacteria	UID2570	433	273	183	7	264	2	0	0	0	96.45	1.09	0
52	o__Flavobacteriales	UID2815	123	324	204	18	294	12	0	0	0	95.81	3.57	41.67
26	k__Bacteria	UID3187	2258	188	117	5	179	4	0	0	0	95.73	2.61	0
0	c__Betaproteobacteria	UID3971	223	424	210	13	404	7	0	0	0	95.24	0.6	85.71
36	o__Burkholderiales	UID4000	193	427	214	40	381	6	0	0	0	95.06	1.82	33.33
79	k__Bacteria	UID203	5449	103	57	3	27	53	20	0	0	94.74	86	52.21
100	k__Bacteria	UID203	5449	104	58	5	40	59	0	0	0	94.67	39.76	5.08
15	f__Xanthomonadaceae	UID4214	55	659	290	60	257	301	38	2	1	94.14	66.99	10.53
22	k__Bacteria	UID2570	433	273	183	16	254	3	0	0	0	93.39	1.37	0
85	k__Bacteria	UID1452	924	161	108	8	151	2	0	0	0	93.06	1.85	0
69	k__Bacteria	UID2570	433	274	183	24	229	19	2	0	0	93.01	8.51	0
27	k__Bacteria	UID1452	924	161	108	10	149	2	0	0	0	92.95	1.03	0
37	c__Betaproteobacteria	UID3959	235	419	211	29	384	6	0	0	0	92.76	1.1	16.67
54	k__Bacteria	UID203	5449	104	58	9	36	58	1	0	0	92.53	56.92	29.51
105	k__Bacteria	UID203	5449	104	58	8	9	14	22	13	38	87.93	210.92	2.78
127	k__Bacteria	UID2982	88	229	147	27	194	8	0	0	0	86.85	3.1	12.5

43	c__Alphaproteobacteria	UID3305	564	349	230	39	307	3	0	0	0	86.77	1.01	33.33
45	f__Flavobacteriaceae	UID2817	81	511	283	69	421	20	1	0	0	85.03	5.74	60.87
4	c__Betaproteobacteria	UID3959	235	413	209	67	291	49	6	0	0	84.16	14	19.4
91	k__Bacteria	UID203	5449	103	57	11	43	46	3	0	0	84.05	50.22	0
50	c__Gammaproteobacteria	UID4267	119	544	284	76	449	19	0	0	0	82.63	3.4	36.84
8	k__Bacteria	UID203	5449	104	58	26	52	19	5	2	0	82.13	36.34	4.35
93	o__Flavobacteriales	UID2815	123	324	204	61	222	38	3	0	0	82.02	11.26	25.53
39	k__Bacteria	UID3187	2258	181	110	36	135	10	0	0	0	78.76	5.78	50
104	o__Burkholderiales	UID4000	193	427	214	102	301	23	1	0	0	77.66	5.52	46.15
111	k__Bacteria	UID2565	2921	143	88	25	113	5	0	0	0	77.56	3.58	0
14	k__Bacteria	UID1452	924	163	110	39	120	4	0	0	0	75.98	2.88	25
124	k__Bacteria	UID1452	924	161	108	39	111	11	0	0	0	75.94	3.86	27.27
110	o__Rhizobiales	UID3654	92	481	319	142	337	2	0	0	0	75.11	0.63	0
46	k__Bacteria	UID203	5449	104	58	32	34	37	0	1	0	74.06	33.86	95.35
84	k__Bacteria	UID1452	924	163	110	51	109	3	0	0	0	71.17	2.73	0
67	k__Bacteria	UID1452	924	163	110	40	120	3	0	0	0	71.09	2	0
64	o__Burkholderiales	UID4105	54	553	264	187	347	18	1	0	0	66.54	4.09	23.81
121	k__Bacteria	UID1452	924	163	110	50	110	3	0	0	0	66.13	1.92	0
59	o__Burkholderiales	UID4000	193	427	214	160	255	12	0	0	0	65.01	2.93	0
2	f__Xanthomonadaceae	UID4214	55	659	290	226	416	17	0	0	0	64.42	2.67	29.41
87	f__Xanthomonadaceae	UID4214	55	659	290	227	427	5	0	0	0	63.45	0.18	80
3	k__Bacteria	UID1452	924	151	101	47	103	1	0	0	0	63.02	0.99	100
33	k__Bacteria	UID1452	924	161	108	51	110	0	0	0	0	61.39	0	0
107	f__Rhodobacteraceae	UID3340	84	568	330	243	267	53	5	0	0	57.5	11.64	16.18
109	k__Bacteria	UID1453	901	171	117	61	92	18	0	0	0	54.36	8.63	66.67
13	c__Betaproteobacteria	UID3971	223	425	211	201	182	42	0	0	0	48.18	9.54	83.33
115	k__Bacteria	UID1452	924	158	106	90	58	10	0	0	0	47.56	7.08	70
112	o__Burkholderiales	UID4000	193	426	214	221	165	39	1	0	0	47.13	9.7	19.05
117	k__Bacteria	UID1452	924	163	110	83	64	16	0	0	0	45.98	5.5	12.5
106	k__Bacteria	UID1452	924	151	101	70	80	1	0	0	0	42.44	0.99	0

58	k__Bacteria	UID203	5449	104	58	71	33	0	0	0	0	41.72	0	0
35	k__Bacteria	UID203	5449	104	58	44	22	19	14	5	0	41.03	22.35	28.57
118	o__Rhizobiales	UID3447	356	416	249	241	127	38	9	1	0	40.03	11.21	1.41
125	k__Bacteria	UID203	5449	104	58	54	24	20	4	0	2	39.67	22.2	26.92
103	k__Bacteria	UID203	5449	104	58	75	27	2	0	0	0	37.54	3.45	0
122	c__Gammaproteobacteria	UID4202	67	481	276	278	147	47	7	0	2	35.63	11.72	24.73
97	k__Bacteria	UID1452	924	163	110	112	40	9	1	1	0	31.73	7.7	0
80	o__Rhodospirillales	UID3754	63	336	201	233	76	22	4	1	0	29.9	8.38	2.5
32	k__Bacteria	UID203	5449	104	58	73	31	0	0	0	0	29.2	0	0
18	k__Bacteria	UID203	5449	104	58	78	23	2	1	0	0	26.21	3.76	20
38	c__Betaproteobacteria	UID3959	235	413	209	297	94	20	2	0	0	20.76	4.87	3.85
49	k__Bacteria	UID203	5449	104	58	82	16	3	3	0	0	20.64	9.35	0
9	k__Bacteria	UID203	5449	104	58	81	23	0	0	0	0	17.95	0	0
12	k__Bacteria	UID203	5449	104	58	88	16	0	0	0	0	15.24	0	0
120	k__Bacteria	UID203	5449	104	58	90	14	0	0	0	0	14.97	0	0
31	k__Bacteria	UID203	5449	100	55	92	8	0	0	0	0	6.28	0	0
96	k__Bacteria	UID203	5449	104	58	96	8	0	0	0	0	5.8	0	0
78	root	UID1	5656	56	24	55	1	0	0	0	0	4.17	0	0
55	root	UID1	5656	56	24	55	1	0	0	0	0	4.17	0	0
10	k__Bacteria	UID203	5449	104	58	101	3	0	0	0	0	2.04	0	0
40	k__Bacteria	UID203	5449	104	58	102	2	0	0	0	0	1.72	0	0
74	k__Archaea	UID2	207	149	107	143	5	1	0	0	0	0.43	0.07	0

Table S2. The 10 most similar genomes of bin0 found using PATRIC.

Genome ID	Genome Name	Contigs	Genome Length	GC Content	Distance	P Value	Counts	NCBI Taxon ID	Genome Status	ANI
1454005.3	*Ca.* Accumulibacter sp. BA-94	299	3097332	63.43	0.106047	8.79E-271	57/1000	1454005	WGS	90.8%
327160.8	*Ca.* Accumulibacter phosphatis strain UBA2327	171	4431027	65.20	0.110193	1.22E-240	52/1000	327160	WGS	88.7%
1454000.3	*Ca.* Accumulibacter sp. SK-11	94	47100180	58.33	0.11197	6.05E-230	50/1000	1454000	WGS	88.5%
2053492.3	*Ca.* Accumulibacter sp. strain UBA8770	406	4010561	65.68	0.112887	1.19E-226	49/1000	2053492	WGS	88.8%
327160.9	*Ca.* Accumulibacter phosphatis strain UBA2315	202	4244559	65.89	0.119909	4.18E-191	42/1000	327160	WGS	88.3%
2053492.4	*Ca.* Accumulibacter sp. strain UBA11070	426	3516715	65.25	0.119909	6.07E-193	42/1000	2053492	WGS	88.7%
327160.12	*Ca.* Accumulibacter phosphatis strain UBA6585	263	4555925	65.75	0.12101	1.60E-185	41/1000	327160	WGS	88.2%
1454001.3	*Ca.* Accumulibacter sp. SK-12	61	4412715	64.57	0.124491	4.67E-171	38/1000	1454001	WGS	88.0%
2053492.6	*Ca.* Accumulibacter sp. strain UBA9001	176	2581832	65.83	0.132399	4.06E-146	32/1000	2053492	WGS	88.5%
522306.3	*Ca.* Accumulibacter phosphatis clade IIA str. UW-1	4	5306133	64.00	0.186761	6.76E-40	10/1000	522306	Complete	84.5%

Table S3. Quality metrics of the "*Ca*. Accumulibacter clade IIF strain SCELSE-1" draft genome.

Characteristics	Values
Genome size (Mbp)	4.25
Contigs	253
Contig N50	26216
Max contig size	100,190
Completeness (%)	95.24
Contamination (%)	0.6
Dominant strains	1
Plasmids	
GC content (%)	66.05
Protein coding density (%)	99
Coding Sequence (CDS)	4023
rRNA copies	1[1]
Abundance: Experiment (by amplicon)	45%

[1] The 16S rRNA gene was recovered using EMIRGE [15].

Table S4 Stoichiometry and kinetics of phosphorus and carbon transformations obtained with different carbon sources in this study and a comparison with literature values and model values for *Ca.* Accumulibacter, *Tetrasphaera* and mixed cultures.

Microorganism	Carbon Source	P/C [a]	PHA/C [b]	PHB/C [c]	PHV/C [d]	PH2MV/C [e]	Propionyl/ Acetyl [f]	Gly/C [g]	P release rate	Carbon uptake rate	P uptake rate	Ref.
		mol P/mol C	mol P/mol C	mol C/mol C	mol C/mol C	mol C/mol C	mol C/mol C	mol C/mol C	mgP/gMLSS/h	mgC/gMLSS/h	mgP/gMLSS/h	
Ca. Accumulibacter Anaerobic P release test	Acetate	0.53	1.37	1.29	0.07	0.01	0.04	- [h]	112.8	81.5	-	This study
	Aspartate	0.24	0.63	0.15	0.35	0.15	0.99	-	21.3	37.4	-	
	Glutamate	0.19	0.05	-	-	-	-	-	18.5	36.5	-	
	Asparagine	0.29	0.74	0.16	0.40	0.17	1.03	-	12.9	31.1	-	
	Glutamine	0.34	0.04	-	-	-	-	-	10.8	24.9	-	
Ca. Accumulibacter Anaerobic-aerobic full cycle study	Acetate	0.51-0.59	1.32-1.34	1.22-1.26	0.11-0.13	0	0.03-0.04	0.43-0.46	112.4-114.8	70.1-74.2	31.5-34.1	This study
	Aspartate	0.28-0.29	0.55-0.59	0.12-0.16	0.32-0.34	0.14-0.16	1.02-1.07	-	17.7-18.0	26.4-29.2	13.4-19.6	
	Glutamate	0.23-0.24	0.02-0.02	-	-	-	-	-	13.3-14.1	20.3-26.1	14.3-17.9	
	Asparagine	0.31-0.36	0.45-0.53	0.11-0.14	0.25-0.26	0.13-0.16	0.96-1.17	-	10.2-10.3	14.1-15.2	6.14-6.19	
	Glutamine	0.36-0.37	0.04-0.04	-	-	-	-	-	9.9-10.0	10.7-10.9	8.25-9.80	
Ca. Accumulibacter In-reactor test	Acetate	0.53	1.35	1.17	0.18	0	0.08	0.41	104.44	82.9	49	This study
	Aspartate	0.29	0.56	0.11	0.47	0.09	1.02	-	19.1	21	30.4	
	Glutamate	0.22	0.03	-	-	-	-	-	10.6	19.8	20.3	
Ca. Accumulibacter - Glycogen model	Acetate	0.5	1.33	1.33	0	0	0	0.5	-	-	-	1

Tetrasphaera elongata	Glycine	0.48	-	-	-	-	-	-	-	-	-	33
Mixed culture	Casein hydrolysate	0.35±0.08	0.15±0.04	0.03±0.01	0.09±0.02	0.03±0.01	-	0.38±0.12	-	-	-	30
Mixed culture	Aspartate	0.29-0.55	0.39-0.95	-	-	-	-	0.55-1.64	-	-	-	31
	Glutamate	0.17-0.73	0.13-0.61	-	-	-	-	0.45-1.24	-	-	-	

[a] P release-to-carbon uptake ratio; [b] PHA formation-to-carbon uptake ratio; [c] PHB formation-to-carbon uptake ratio; [d] PHV formation-to-carbon uptake ratio; [e] PH2MV formation-to-carbon uptake ratio; [f] the ratio of the propionyl- and acetyl- residues in PHA; [g] Glycogen consumption-to-carbon uptake ratio; [h] not available.

Table S5 Key genes and the encoding enzymes potentially involved in amino acid metabolism in *Ca.* Accumulibacter clade IIF strain SCELSE-1, their homologous genes in *Ca.* Accumulibacter clade IIA strain UW-1 and their expression patterns as in Oyserman et al., 2016. [34] Detailed expression profiles are shown in Fig. S11.

Feature ID	Type	Function	Ontology	Start	Strand	Length	Contig	Homologue in Clade IIA strain UW-1	Expression patterns [34]
gAccumu.CDS.1221	gene	Acetate permease ActP (cation/acetate symporter)	SSO:000000671- Acetate permease ActP (cation/acetate symporter)	19,034	+	1,662	contig-100_201	CAP2UW1_1608	An↑Ae↓[a]
gAccumu.CDS.1941	gene	Acetate permease ActP (cation/acetate symporter)	SSO:000000671- Acetate permease ActP (cation/acetate symporter)	24,440	+	2,037	contig-100_601	CAP2UW1_3752	An↓Ae↑[b]
gAccumu.CDS.3048	gene	Acetate kinase (EC 2.7.2.1)	SSO:000000670- Acetate kinase (EC 2.7.2.1)	27,859	+	1,185	contig-100_815	CAP2UW1_1515	An↑Ae↓
gAccumu.CDS.2188	gene	Polyphosphate kinase (EC 2.7.4.1)	SSO:000006159- Polyphosphate kinase (EC 2.7.4.1)	6,490	-	2,121	contig-100_2131	CAP2UW1_1063	An↑Ae↓
gAccumu.CDS.1743	gene	Exopolyphosphatase (EC 3.6.1.11)	SSO:000002629- Exopolyphosphatase (EC 3.6.1.11)	42,196	+	1,533	contig-100_139	CAP2UW1_1064	An↑Ae↓
gAccumu.CDS.2189_CDS	CDS	Exopolyphosphatase (EC 3.6.1.11)	SSO:000002629- Exopolyphosphatase (EC 3.6.1.11)	6,725	+	1,533	contig-100_2131	CAP2UW1_0060	An↑Ae→ [c]
gAccumu.CDS.2491	gene	Polyphosphate kinase 2 (EC 2.7.4.1)		10,460	+	1,059	contig-100_3027	CAP2UW1_2309	An↑Ae↓
gAccumu.CDS.3872	gene	Polyphosphate kinase 2 (EC 2.7.4.1)		13,824	-	1,260	contig-100_1653	CAP2UW1_3622	An↓Ae↑
gAccumu.CDS.2826	gene	Polyhydroxyalkanoic acid synthase		19,505	-	702	contig-100_1811	CAP2UW1_3185	An↑Ae→

gAccumu.CDS.1702	gene	polyhydroxyalkanoate granule-associated protein PhaI	95,102	-	594	contig-100_130	CAP2UW1_3347	No specific pattern
gAccumu.CDS.582	gene	Polyhydroxyalkanoic acid synthase	8,015	-	1,107	contig-100_2807	CAP2UW1_4338	No specific pattern
gAccumu.CDS.589	gene	Polyhydroxyalkanoic acid synthase	12,793	+	1,389	contig-100_2807	CAP2UW1_3191	An↑Ae↓
gAccumu.CDS.3876	gene	Anaerobic C4-dicarboxylate transporter	20,516	-	1,326	contig-100_1653	CAP2UW1_1862	An↑Ae↓
gAccumu.CDS.1796	gene	Glutamate Aspartate periplasmic binding protein precursor GltI (TC 3.A.1.3.4)	87,897	+	1,023	contig-100_139	CAP2UW1_4241	An ○ Ae→[d]
gAccumu.CDS.2218	gene	Glutamate Aspartate periplasmic binding protein precursor GltI (TC 3.A.1.3.4)	13,329	+	906	contig-100_1434	CAP2UW1_1834	No specific pattern
gAccumu.CDS.3568	gene	Glutamate Aspartate periplasmic binding protein precursor GltI (TC 3.A.1.3.4)	6,506	+	906	contig-100_2495	CAP2UW1_1092	An↓Ae↑
gAccumu.CDS.3569	gene	Glutamate Aspartate transport system permease protein GltJ (TC 3.A.1.3.4)	7,471	+	741	contig-100_2495	CAP2UW1_1094	An ○ Ae→
gAccumu.CDS.3570	gene	Glutamate Aspartate transport system permease protein GltK (TC 3.A.1.3.4)	8,213	+	681	contig-100_2495	CAP2UW1_1095	An↓Ae→[e]
gAccumu.CDS.3571	gene	Glutamate Aspartate transport ATP-binding protein GltL (TC 3.A.1.3.4)	9,029	+	729	contig-100_2495	CAP2UW1_1096	An↓Ae→

gAccumu.CDS.4435	gene	Glutamate Aspartate periplasmic binding protein precursor GltI (TC 3.A.1.3.4)		23,422	-	858	contig-100_507	CAP2UW1_2891	An ○ Ae→
gAccumu.CDS.3841	gene	L-asparaginase (EC 3.5.1.1)	SSO:000004125- L-asparaginase (EC 3.5.1.1)	570	+	1,068	contig-100_23642	CAP2UW1_1093	An ○ Ae↑[f]
gAccumu.CDS.88	gene	L-aspartate oxidase (EC 1.4.3.16)	SSO:000004128- L-aspartate oxidase (EC 1.4.3.16)	38,182	-	1,575	contig-100_479	CAP2UW1_1542	An↑Ae↓
gAccumu.CDS.1129	gene	Phosphoenolpyruvate carboxykinase [GTP] (EC 4.1.1.32)	SSO:000005954- Phosphoenolpyruvate carboxykinase [GTP] (EC 4.1.1.32)	7,169	-	1,839	contig-100_1711	CAP2UW1_0771	An↑Ae↓
MEIGNLFM_01607	gene	Phosphoenolpyruvate carboxykinase [GTP]	SSO:000005954- Phosphoenolpyruvate carboxykinase [GTP] (EC 4.1.1.32)	77,418	+	627	contig-100_139	CAP2UW1_1298	An↑Ae↓
gAccumu.CDS.2372	gene	Pyruvate kinase (EC 2.7.1.40)	SSO:000006852- Pyruvate kinase (EC 2.7.1.40)	3,889	+	1,440	contig-100_4523	CAP2UW1_0821	An↑Ae↓
gAccumu.CDS.3499	gene	Pyruvate kinase (EC 2.7.1.40)	SSO:000006852- Pyruvate kinase (EC 2.7.1.40)	14,030	-	1,413	contig-100_248	CAP2UW1_1890	An ○ Ae→
gAccumu.CDS.4085	gene	Pyruvate dehydrogenase E1 component (EC 1.2.4.1)	SSO:000006847- Pyruvate dehydrogenase E1 component (EC 1.2.4.1)	11,997	-	2,694	contig-100_517	CAP2UW1_1838	An ○ Ae↑
gAccumu.CDS.3526	gene	Aspartate ammonia-lyase	SSO:000001094- Aspartate ammonia-lyase (EC 4.3.1.1)	20,939	-	321	contig-100_1653	CAP2UW1_3016	An↓Ae→
gAccumu.CDS.1073	gene	Adenylosuccinate synthetase (EC 6.3.4.4)	SSO:000000824- Adenylosuccinate synthetase (EC 6.3.4.4)	2,587	-	1,308	contig-100_953	CAP2UW1_2911	An↑Ae↓
gAccumu.CDS.1821	gene	Adenylosuccinate lyase (EC 4.3.2.2)	SSO:000000823- Adenylosuccinate lyase (EC 4.3.2.2)	9,294	+	1,368	contig-100_3701	CAP2UW1_2523	An↑Ae↓

gAccumu.CDS.1945	gene	Diaminohydroxyphosphoribosylaminopyrimidine deaminase (EC 3.5.4.26) / 5-amino-6-(5-phosphoribosylamino)uracil reductase (EC 1.1.1.193)	SSO:000000412- 5-amino-6-(5-phosphoribosylamino)uracil reductase (EC 1.1.1.193)SSO:000002279- Diaminohydroxyphosphoribosylaminopyrimidine deaminase (EC 3.5.4.26)	28,716	+	1,107	contig-100_601	CAP2UW1_1500	An↑Ae↓
gAccumu.CDS.608	gene	Argininosuccinate lyase (EC 4.3.2.1)	SSO:000001051- Argininosuccinate lyase (EC 4.3.2.1)	14,867	+	1,389	contig-100_1523	CAP2UW1_0789	An↑Ae↓
gAccumu.CDS.2478	gene	Argininosuccinate synthase (EC 6.3.4.5)	SSO:000001052- Argininosuccinate synthase (EC 6.3.4.5)	6,965	-	1,230	contig-100_4260	CAP2UW1_3083	An↑Ae↓
gAccumu.CDS.2479	gene	Ornithine carbamoyltransferase (EC 2.1.3.3)	SSO:000005514- Ornithine carbamoyltransferase (EC 2.1.3.3)	7,915	-	954	contig-100_4260	CAP2UW1_3084	An↑Ae↓
gAccumu.CDS.4026	gene	Fumarate reductase subunit C	SSO:000002960- Fumarate reductase subunit C	1,229	+	399	contig-100_1021	CAP2UW1_0924	An↑Ae↑ [g]
gAccumu.CDS.4027	gene	Fumarate reductase subunit D	SSO:000002961- Fumarate reductase subunit D	1,624	+	369	contig-100_1021	CAP2UW1_0923	An↑Ae→
gAccumu.CDS.1	gene	Succinate dehydrogenase iron-sulfur protein (EC 1.3.99.1)	SSO:000007781- Succinate dehydrogenase iron-sulfur protein (EC 1.3.99.1)	56	+	714	contig-100_9384	CAP2UW1_2385	An↑Ae↓
gAccumu.CDS.3082	gene	Succinate dehydrogenase flavoprotein subunit (EC 1.3.99.1)	SSO:000007779- Succinate dehydrogenase flavoprotein subunit (EC 1.3.99.1)	13,034	+	1,785	contig-100_2630	CAP2UW1_2384	An↑Ae↓

gAccumu.CDS.1533	gene	Succinyl-CoA ligase [ADP-forming] beta chain (EC 6.2.1.5)	SSO:000007790- Succinyl-CoA ligase [ADP-forming] beta chain (EC 6.2.1.5)	23	+	1,161	contig-100_4567	CAP2UW1_0656	An↑Ae↓
gAccumu.CDS.1382	gene	Succinate--CoA ligase [ADP-forming] subunit alpha	SSO:000001032- Archaeal succinyl-CoA ligase [ADP-forming] alpha	1194	+	894	contig-100_4567	CAP2UW1_0657	An↑Ae↓
gAccumu.CDS.1757	gene	Methylmalonyl-CoA mutase (EC 5.4.99.2)	SSO:000004891- Methylmalonyl-CoA mutase (EC 5.4.99.2)	57,589	+	2,175	contig-100_139	CAP2UW1_1139	An↑Ae↓
gAccumu.CDS.1760	gene	Methylmalonyl-CoA decarboxylase	SSO:000004886- Methylmalonyl-CoA decarboxylase, alpha chain (EC 4.1.1.41)	52,159	+	780	contig-100_256	CAP2UW1_3914	An O Ae→
gAccumu.CDS.877	gene	Oxaloacetate decarboxylase beta chain (EC 4.1.1.3) / Methylmalonyl-CoA decarboxylase, beta chain (EC 4.1.1.41)	SSO:000004887- Methylmalonyl-CoA decarboxylase, beta chain (EC 4.1.1.41) SSO:000005616- Oxaloacetate decarboxylase beta chain (EC 4.1.1.3)	5,017	-	1,209	contig-100_9049	CAP2UW1_3917	An O Ae→
gAccumu.CDS.3572	gene	NAD-specific glutamate dehydrogenase (EC 1.4.1.2), large form		9,943	+	4,659	contig-100_2495	CAP2UW1_1097	An↑Ae↑
gAccumu.CDS.2080	gene	Arginine decarboxylase (EC 4.1.1.19), Ornithine decarboxylase (EC 4.1.1.17), Lysine decarboxylase (EC 4.1.1.18)	SSO:000001044- Arginine decarboxylase (EC 4.1.1.19) SSO:000004598- Lysine decarboxylase (EC 4.1.1.18) SSO:000005516- Ornithine decarboxylase (EC 4.1.1.17)	6,458	-	1,542	contig-100_9027	CAP2UW1_4030	An↑Ae↓

gAccumu.CDS.1683	gene	Isocitrate dehydrogenase [NADP] (EC 1.1.1.42)	SSO:000004050- Isocitrate dehydrogenase [NADP] (EC 1.1.1.42)	75,772	+	1,230	contig-100_130	CAP2UW1_0663	An↑Ae↓
gAccumu.CDS.2722	gene	Ketoglutarate oxidoreductase, beta subunit (EC 1.2.7.3)	SSO:000000208- Ketoglutarate oxidoreductase, beta subunit (EC 1.2.7.3)	2,765	-	1,056	contig-100_5269	CAP2UW1_2584	An↑Ae↓
gAccumu.CDS.2723	gene	Ketoglutarate oxidoreductase, alpha subunit (EC 1.2.7.3)	SSO:000000207- Ketoglutarate oxidoreductase, alpha subunit (EC 1.2.7.3)	4,605	-	1,839	contig-100_5269	CAP2UW1_2583	An↑Ae↓
gAccumu.CDS.2855	gene	Glutamine synthetase type I (EC 6.3.1.2)	SSO:000003172- Glutamine synthetase type I (EC 6.3.1.2)	27,066	-	1,416	contig-100_649	CAP2UW1_0248	An↑Ae↓
gAccumu.CDS.2506	gene	CTP synthase (glutamine hydrolysing) (EC 6.3.4.2)	SSO:000001378- CTP synthase (EC 6.3.4.2)	13,554	-	1,689	contig-100_2230	CAP2UW1_3327	An↑Ae↓
gAccumu.CDS.2539	gene	Gamma-glutamyltranspeptidase (EC 2.3.2.2)	SSO:000003036- Gamma-glutamyltranspeptidase (EC 2.3.2.2)	1,736	+	1,644	contig-100_1364	CAP2UW1_1179	An O Ae→
gAccumu.CDS.2240	gene	Gamma-glutamyltranspeptidase (EC 2.3.2.2)	SSO:000003036- Gamma-glutamyltranspeptidase (EC 2.3.2.2)	13,652	-	1,944	contig-100_762	CAP2UW1_0230	An↑Ae↓
gAccumu.CDS.2746	gene	Capsule biosynthesis protein CapA		4,835	-	987	contig-100_1283	CAP2UW1_0829	An↑Ae↓
gAccumu.CDS.988	gene	Actin cross-linking toxin VgrG1	SSO:000006139- Poly-gamma-glutamate synthase subunit PgsA/CapA (EC 6.3.2.-) SSO:000006140- Poly-gamma-glutamate synthase subunit PgsB/CapB (EC	4683	+	687	contig-100_7042	--	--[h]

			6.3.2.-) SSO:000006141- Poly-gamma-glutamate synthase subunit PgsC/CapC (EC 6.3.2.-) SSO:000006142- Poly-gamma-glutamate synthase subunit PgsE/CapE (EC 6.3.2.-)						
gAccumu.CDS.1933	gene	Glutamate racemase (EC 5.1.1.3)	SSO:000003153- Glutamate racemase (EC 5.1.1.3)	16,497	-	786	contig-100_601	CAP2UW1_3759	An↑Ae↓
gAccumu.CDS.3930	gene	Dihydrofolate synthase/folylpolyglutamate synthase	SSO:000002289- Dihydrofolate synthase (EC 6.3.2.12)	49,167	-	1,335	contig-100_187	CAP2UW1_1233	An↑Ae↓

[a] anaerobic increase, aerobic decrease; [b] anaerobic decrease, aerobic increase; [c] anaerobic increase, aerobic high expression; [d] anaerobic no specific pattern, aerobic high expression; [e] anaerobic decrease, aerobic high expression; [f] anaerobic no specific pattern, aerobic increase; [g] anaerobic increase, aerobic increase; [h] not found.

Table S6 Reactions involved in the amino acid metabolism as identified in the metagenomic analysis.

Reaction code	Name	Equation	Genes involved
rxn10042[c0]	F(1)-ATPase	ADP[c0] + Phosphate[c0] + (4) H^+[e0] <=> H_2O[c0] + ATP[c0] + (3) H^+[c0]	gAccumu.CDS.1172_CDS, gAccumu.CDS.1172, gAccumu.CDS.1171, gAccumu.CDS.1171_CDS, gAccumu.CDS.960, gAccumu.CDS.960_CDS, gAccumu.CDS.1176, gAccumu.CDS.1176_CDS, gAccumu.CDS.1169, gAccumu.CDS.1169_CDS, gAccumu.CDS.961, gAccumu.CDS.961_CDS, gAccumu.CDS.1170_CDS, gAccumu.CDS.1170
rxn05312[c0]	Inorganic phosphate transporter	Phosphate[e0] + H^+[e0] <= Phosphate[c0] + H^+[c0]	gAccumu.CDS.4119, gAccumu.CDS.708_CDS, gAccumu.CDS.4119_CDS, gAccumu.CDS.4310_CDS, gAccumu.CDS.4113, gAccumu.CDS.708, gAccumu.CDS.4310, gAccumu.CDS.4113_CDS
rxn10151[c0]	TRANS-RXN-122A.cp	L-Aspartate[e0] + (2) H^+[e0] <=> L-Aspartate[c0] + (2) H^+[c0]	gAccumu.CDS.2142, gAccumu.CDS.2142_CDS

rxn05152[c0]	ATP phosphohydrolase (polar-amino-acid-importing)	H_2O[c0] + ATP[c0] + L-Aspartate[e0] => ADP[c0] + Phosphate[c0] + L-Aspartate[c0] + H^+[c0]	gAccumu.CDS.3569_CDS, gAccumu.CDS.3569, gAccumu.CDS.3571_CDS, gAccumu.CDS.3571, gAccumu.CDS.3570_CDS, gAccumu.CDS.3570, gAccumu.CDS.3568_CDS, gAccumu.CDS.1796_CDS, gAccumu.CDS.1796, gAccumu.CDS.2218, gAccumu.CDS.2218_CDS, gAccumu.CDS.4435, gAccumu.CDS.4435_CDS, gAccumu.CDS.893_CDS, gAccumu.CDS.893, gAccumu.CDS.3568
rxn00347[c0]	L-Aspartate ammonia-lyase	L-Aspartate[c0] <=> NH_3[c0] + Fumarate[c0]	gAccumu.CDS.3877, gAccumu.CDS.2353_CDS, gAccumu.CDS.3877_CDS, gAccumu.CDS.2353
rxn00262[c0]	L-Aspartic acid: oxygen oxidoreductase (deaminating)	H_2O[c0] + O_2[c0] + L-Aspartate[c0] => NH_3[c0] + H_2O_2[c0] + Oxaloacetate[c0]	gAccumu.CDS.88, gAccumu.CDS.88_CDS
rxn00305[c0]	GTP:oxaloacetate carboxy-lyase (adding GTP;phosphoenolpyruvate-forming)	Oxaloacetate[c0] + GTP[c0] => CO_2[c0] + GDP[c0] + Phosphoenolpyruvate[c0]	gAccumu.CDS.1129_CDS, gAccumu.CDS.1129, gAccumu.CDS.1780_CDS, gAccumu.CDS.1780, gAccumu.CDS.793, gAccumu.CDS.793_CDS

rxn00148[c0]	ATP: pyruvate 2-O-phosphotransferase	ATP[c0] + Pyruvate[c0] <=> ADP[c0] + Phosphoenolpyruvate[c0] + H^+[c0]	gAccumu.CDS.2372, gAccumu.CDS.3499_CDS, gAccumu.CDS.3499, gAccumu.CDS.2372_CDS
rxn00162[c0]	Oxaloacetate carboxy-lyase (pyruvate-forming)	Oxaloacetate[c0] + H^+[c0] => CO_2[c0] + Pyruvate[c0]	gAccumu.CDS.877, gAccumu.CDS.877_CDS
rxn00148[c0]	ATP: pyruvate 2-O-phosphotransferase	ATP[c0] + Pyruvate[c0] <=> ADP[c0] + Phosphoenolpyruvate[c0] + H^+[c0]	gAccumu.CDS.2372, gAccumu.CDS.3499_CDS, gAccumu.CDS.3499, gAccumu.CDS.2372_CDS
rxn05938[c0]	Pyruvate ferredoxin oxidoreductase	CO_2[c0] + Acetyl-CoA[c0] + H^+[c0] + Reducedferredoxin[c0] <=> CoA[c0] + Pyruvate[c0] + Oxidizedferredoxin[c0]	gAccumu.CDS.962_CDS, gAccumu.CDS.962, gAccumu.CDS.391, gAccumu.CDS.391_CDS
rxn09272[c0]	Fumarate reductase complex (i.e. FRD, involved in anaerobic respiration, repressed in aerobic respiration)	Succinate[c0] + Ubiquinone-8[c0] <=> Fumarate[c0] + Ubiquinol-8[c0]	gAccumu.CDS.3082_CDS, gAccumu.CDS.3930_CDS, gAccumu.CDS.3930, gAccumu.CDS.4024_CDS, gAccumu.CDS.4024, gAccumu.CDS.3082, gAccumu.CDS.3080, gAccumu.CDS.3080_CDS, gAccumu.CDS.4026_CDS, gAccumu.CDS.4026, gAccumu.CDS.4027_CDS, gAccumu.CDS.4027, gAccumu.CDS.3081_CDS, gAccumu.CDS.3081, gAccumu.CDS.4025_CDS,

			gAccumu.CDS.4025, gAccumu.CDS.1, gAccumu.CDS.1_CDS
rxn00285[c0]	Succinate: CoA ligase (ADP-forming)	ATP[c0] + CoA[c0] + Succinate[c0] <=> ADP[c0] + Phosphate[c0] + Succinyl-CoA[c0]	gAccumu.CDS.1533_CDS, gAccumu.CDS.1533, gAccumu.CDS.1534_CDS, gAccumu.CDS.1534
rxn00672[c0]	(S)-methylmalonyl-CoA carboxy-lyase (propanoyl-CoA-forming)	H^+[c0] + D-methylmalonyl-CoA[c0] => CO_2[c0] + Propionyl-CoA[c0]	gAccumu.CDS.877_CDS, gAccumu.CDS.877
rxn00194[c0]	L-glutamate 1-carboxy-lyase (4-aminobutanoate-forming)	L-Glutamate[c0] + H+[c0] => CO_2[c0] + GABA[c0]	gAccumu.CDS.251, gAccumu.CDS.251_CDS, gAccumu.CDS.2080_CDS, gAccumu.CDS.2080
rxn02792[c0]	Gamma-glutamyltranspeptidase family protein	L-Glutamate[c0] + H^+[c0] + L-3-Cyanoalanine[c0] => H_2O[c0] + CO_2[c0] + gamma-Glutamyl-3-aminopropiononitrile[c0]	gAccumu.CDS.2539, gAccumu.CDS.2240, gAccumu.CDS.2539_CDS, gAccumu.CDS.2240_CDS
rxn00193[c0]	Glutamate racemase	L-Glutamate[c0] <=> D-Glutamate[c0]	gAccumu.CDS.1933_CDS, gAccumu.CDS.1933, gAccumu.CDS.138_CDS, gAccumu.CDS.138

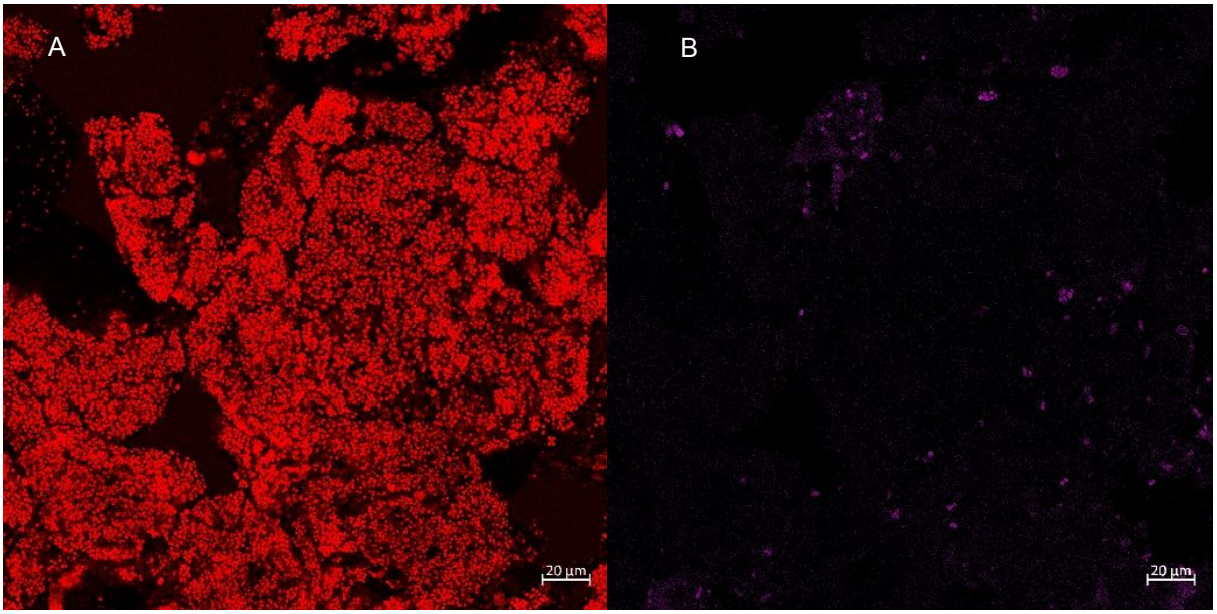

298

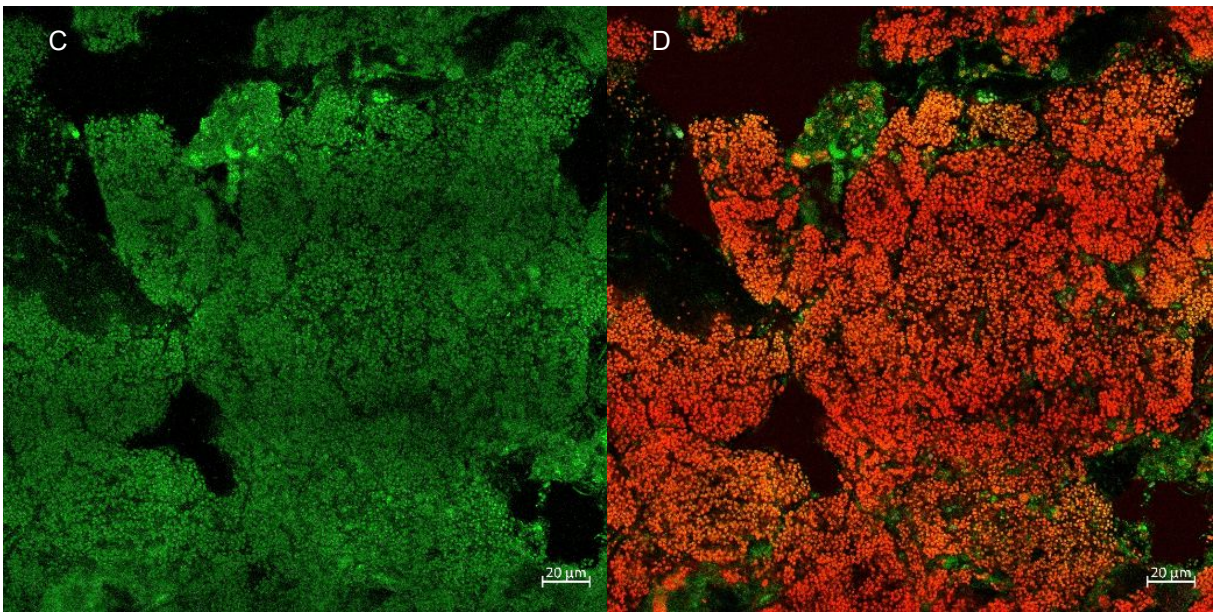

299

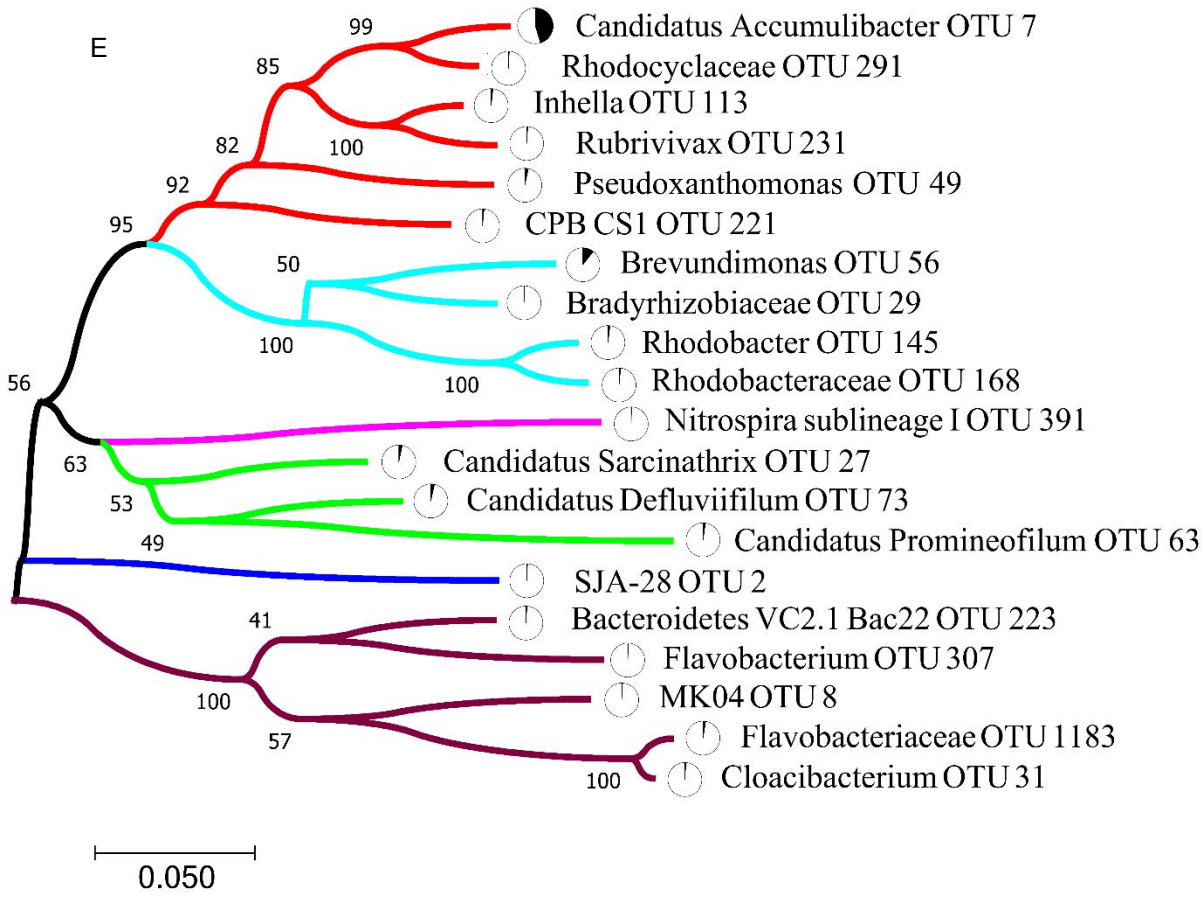

Figure S1 PAOs and GAOs visualized by FISH imaging and microbial community composition analysis based on 16S rRNA gene amplicon sequencing of the enrichment culture in the SBR. (**A)** *Ca.* Accumulibacter targeted by PAOmix; (**B)** *Competibacter*-related GAOs targeted by GAOmix; (**C)** Most bacteria targeted by EUBmix; (**D)** Superimposed images of A, B and C; and (**E**) Phylogenetic tree of the OTUs present (97% identity) in the enrichment culture based on 16S rRNA gene amplicon analysis (only OTUs with relative abundance >0.5% are shown; the pie charts at the end of each branch indicate the relative abundance of the OTU). A single OTU of *Ca.* Accumulibacter, strain SCELSE-1, dominated the community (Day 152).

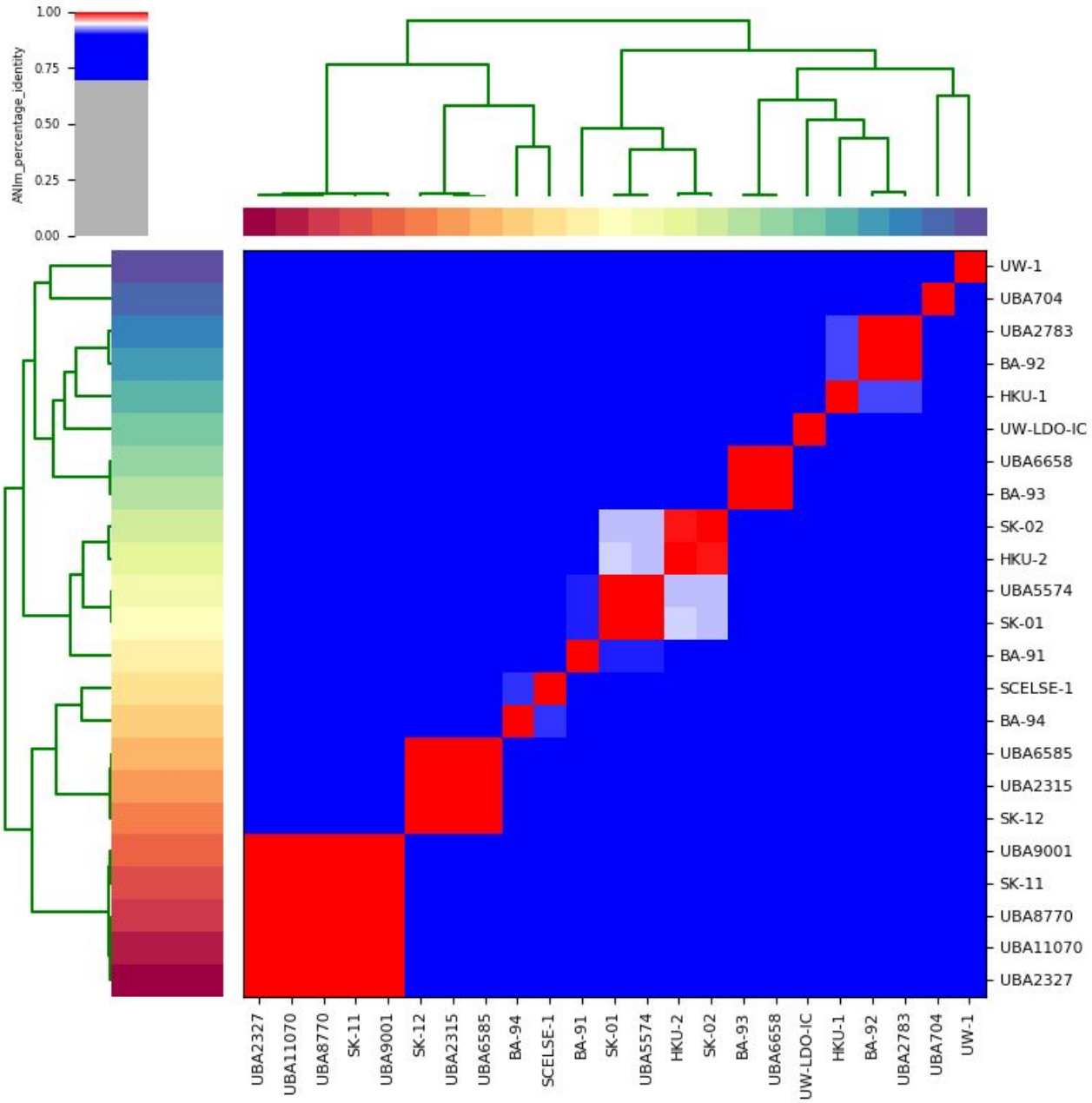

Figure S2 Comparison of the genome-wide average nucleotide identities (ANI) of *Ca.* Accumulibacter genomes.

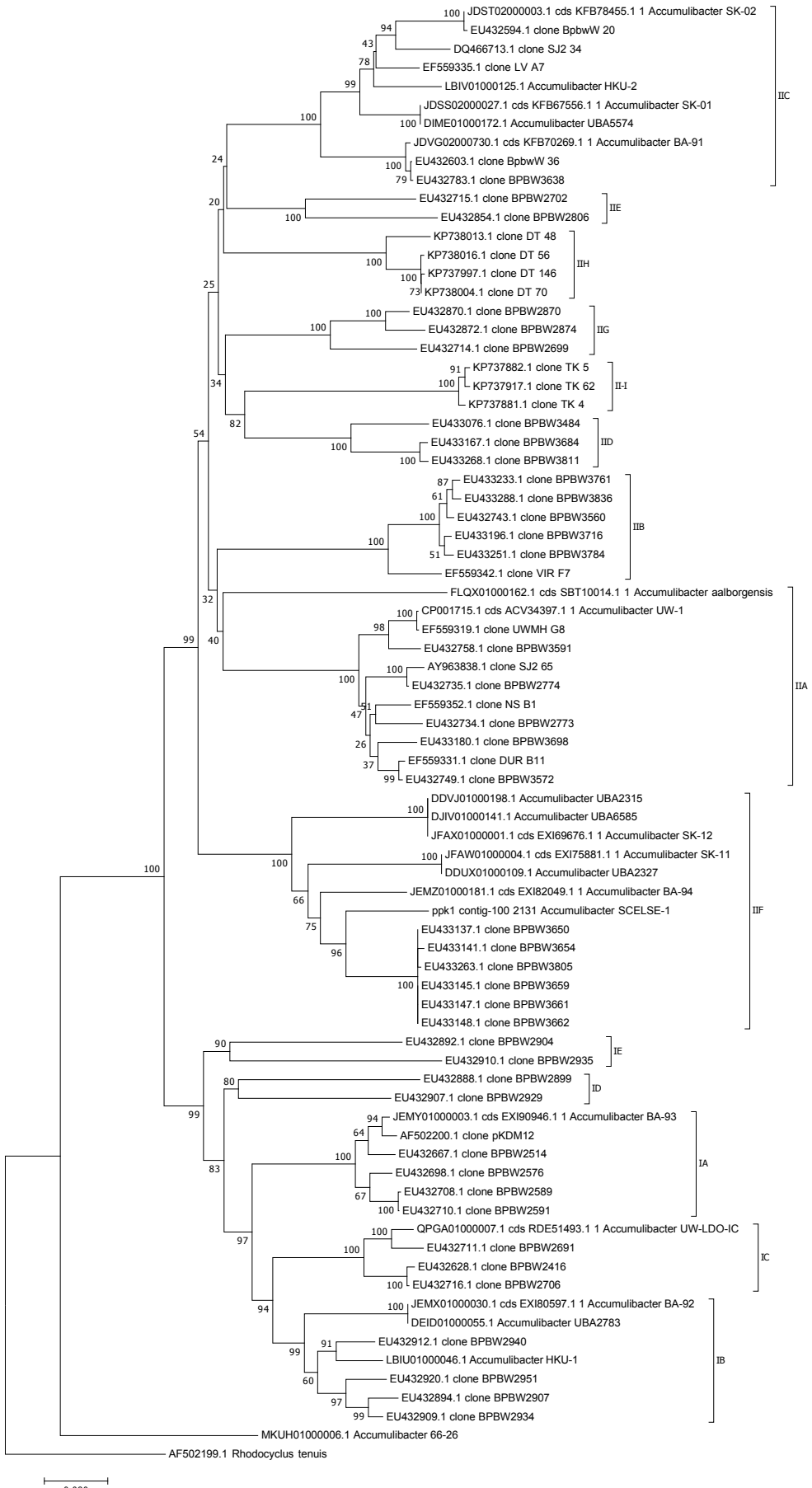
JDST02000003.1 cds KFB78455.1 1 Accumulibacter SK-02
EU432594.1 clone BpbwW 20
DQ466713.1 clone SJ2 34
EF559335.1 clone LV A7
LBIV01000125.1 Accumulibacter HKU-2
JDSS02000027.1 cds KFB67556.1 1 Accumulibacter SK-01
DIME01000172.1 Accumulibacter UBA5574
JDVG02000730.1 cds KFB70269.1 1 Accumulibacter BA-91
EU432603.1 clone BpbwW 36
EU432783.1 clone BPBW3638
IIC
EU432715.1 clone BPBW2702
EU432854.1 clone BPBW2806
IIE
KP738013.1 clone DT 48
KP738016.1 clone DT 56
KP737997.1 clone DT 146
KP738004.1 clone DT 70
IIH
EU432870.1 clone BPBW2870
EU432872.1 clone BPBW2874
EU432714.1 clone BPBW2699
IIG
KP737882.1 clone TK 5
KP737917.1 clone TK 62
KP737881.1 clone TK 4
II-I
EU433076.1 clone BPBW3484
EU433167.1 clone BPBW3684
EU433268.1 clone BPBW3811
IID
EU433233.1 clone BPBW3761
EU433288.1 clone BPBW3836
EU432743.1 clone BPBW3560
EU433196.1 clone BPBW3716
EU433251.1 clone BPBW3784
EF559342.1 clone VIR F7
IIB
FLQX01000162.1 cds SBT10014.1 1 Accumulibacter aalborgensis
CP001715.1 cds ACV34397.1 1 Accumulibacter UW-1
EF559319.1 clone UWMH G8
EU432758.1 clone BPBW3591
AY963838.1 clone SJ2 65
EU432735.1 clone BPBW2774
EF559352.1 clone NS B1
EU432734.1 clone BPBW2773
EU433180.1 clone BPBW3698
EF559331.1 clone DUR B11
EU432749.1 clone BPBW3572
IIA
DDVJ01000198.1 Accumulibacter UBA2315
DJIV01000141.1 Accumulibacter UBA6585
JFAX01000001.1 cds EXI69676.1 1 Accumulibacter SK-12
JFAW01000004.1 cds EXI75881.1 1 Accumulibacter SK-11
DDUX01000109.1 Accumulibacter UBA2327
JEMZ01000181.1 cds EXI82049.1 1 Accumulibacter BA-94
ppk1 contig-100 2131 Accumulibacter SCELSE-1
EU433137.1 clone BPBW3650
EU433141.1 clone BPBW3654
EU433263.1 clone BPBW3805
EU433145.1 clone BPBW3659
EU433147.1 clone BPBW3661
EU433148.1 clone BPBW3662
IIF
EU432892.1 clone BPBW2904
EU432910.1 clone BPBW2935
IIE
EU432888.1 clone BPBW2899
EU432907.1 clone BPBW2929
IID
JEMY01000003.1 cds EXI90946.1 1 Accumulibacter BA-93
AF502200.1 clone pKDM12
EU432667.1 clone BPBW2514
EU432698.1 clone BPBW2576
EU432708.1 clone BPBW2589
EU432710.1 clone BPBW2591
IA
QPGA01000007.1 cds RDE51493.1 1 Accumulibacter UW-LDO-IC
EU432711.1 clone BPBW2691
EU432628.1 clone BPBW2416
EU432716.1 clone BPBW2706
IC
JEMX01000030.1 cds EXI80597.1 1 Accumulibacter BA-92
DEID01000055.1 Accumulibacter UBA2783
EU432912.1 clone BPBW2940
LBIU01000046.1 Accumulibacter HKU-1
EU432920.1 clone BPBW2951
EU432894.1 clone BPBW2907
EU432909.1 clone BPBW2934
IB
MKUH01000006.1 Accumulibacter 66-26
AF502199.1 Rhodocyclus tenuis
0.020

Figure S3 Neighbor-joining phylogenetic tree based on nucleotide sequences of *ppk1* found in clones and genomes of *Ca*. Accumulibacter. Sequences were aligned in MEGA7 [35] applying a Muscle alignment with default settings. Sequences were trimmed giving an alignment length of 1006 bp.

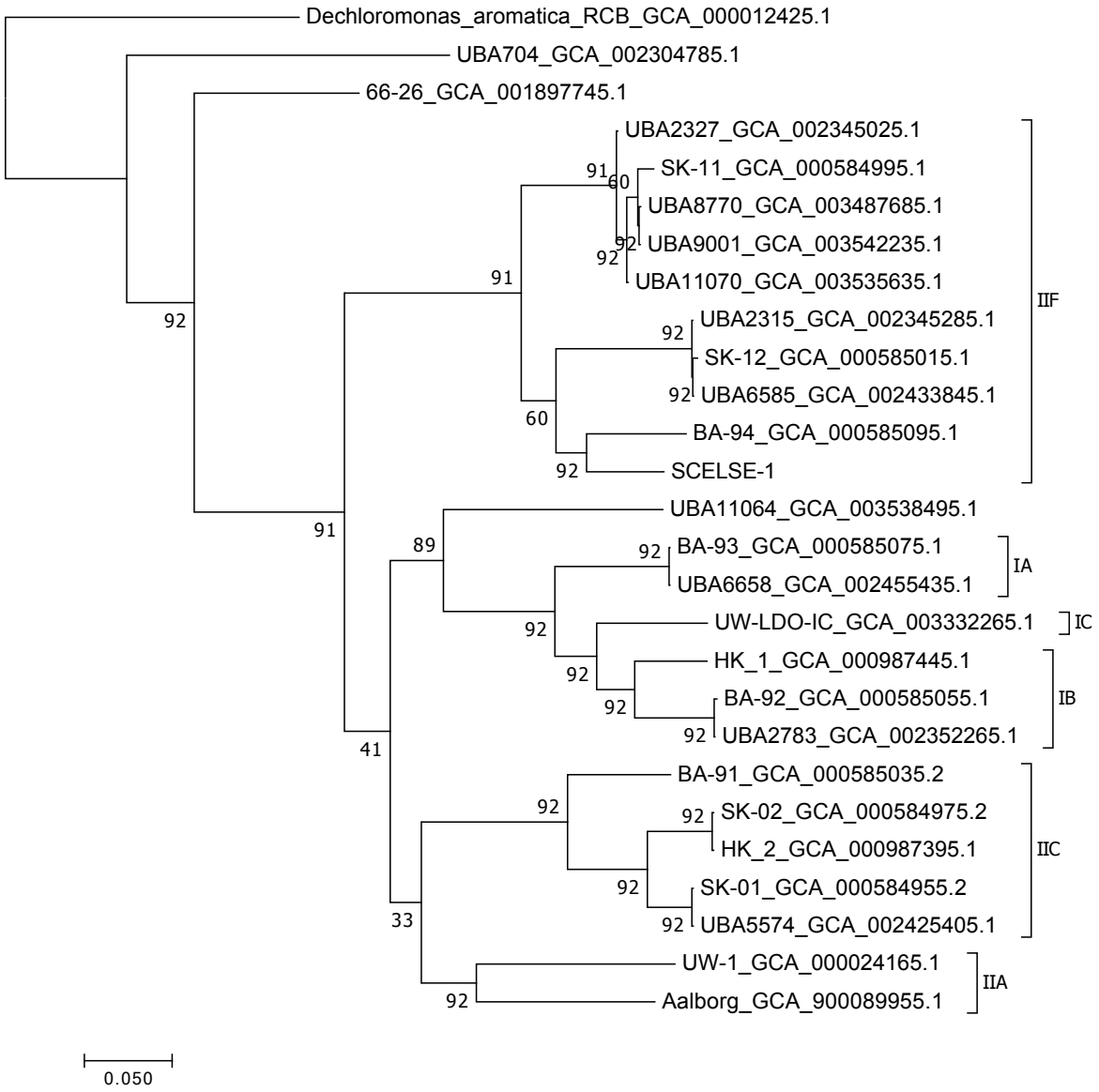

Figure S4 Phylogenetic tree of a concatenated alignment of 92 maker genes for *Ca.* Accumulibacter draft genomes published in GeneBank using the UBCG pipeline [19].

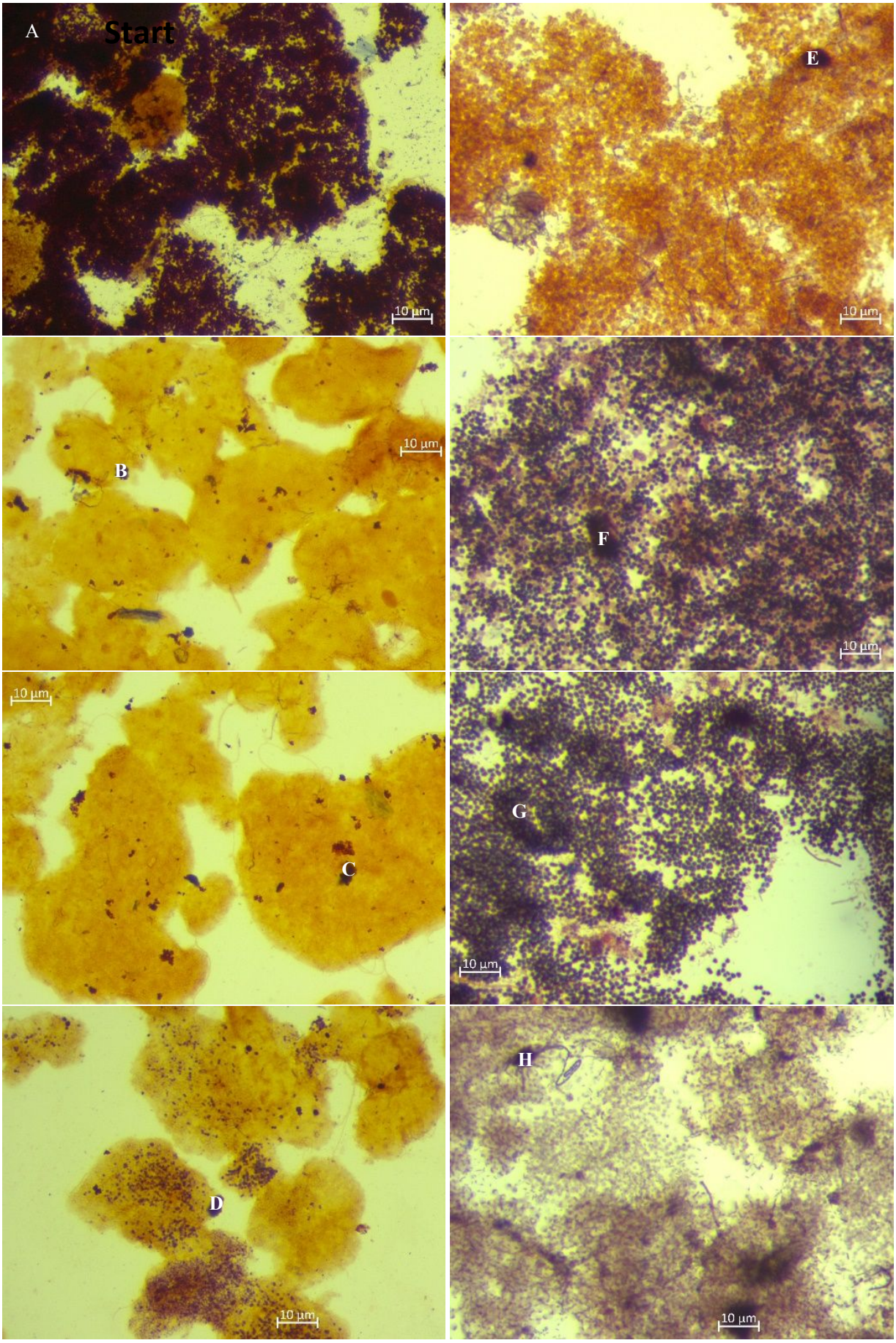
A
Start
10 µm
E
10 µm
B
10 µm
F
10 µm
10 µm
C
G
10 µm
D
10 µm
H
10 µm

Figure S5 P-release and PHA formation behaviors when amino acids were used as carbon sources as compared to acetate. Poly-P was stained using methylene blue (**A**. state before experiment, **B**. after anaerobic incubation with acetate for 10 h, **C**. after anaerobic incubation with aspartate for10 h, **D**. after anaerobic incubation with glutamine for 10 h). PHA was stained using Sudan black (**E**. state before experiment, **F**. after anaerobic incubation with acetate for 10 h, **G**. after anaerobic incubation with aspartate for10 h, **H**. after anaerobic incubation with glutamine for 10 h). Chemical staining was performed according to Nielsen et al.[36]

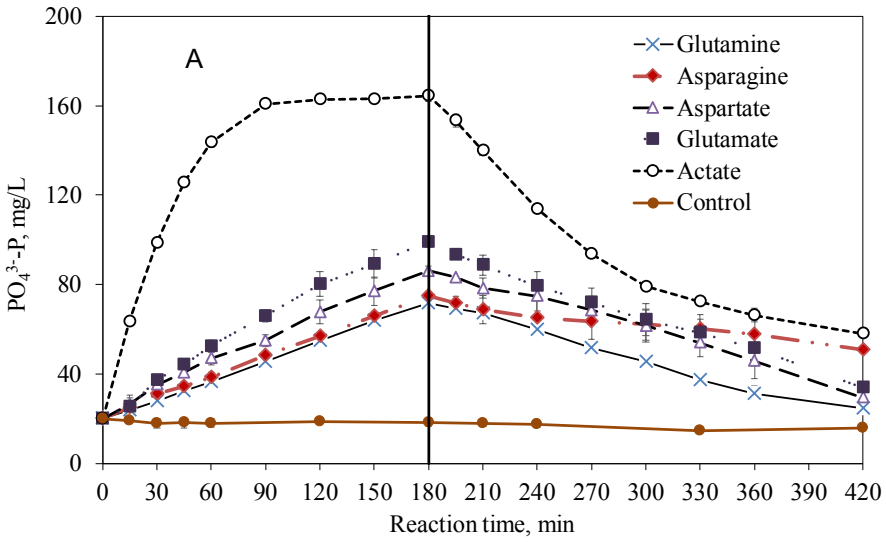
A
Glutamine
Asparagine
Aspartate
Glutamate
Actate
Control
PO_4^{3-}-P, mg/L
Reaction time, min

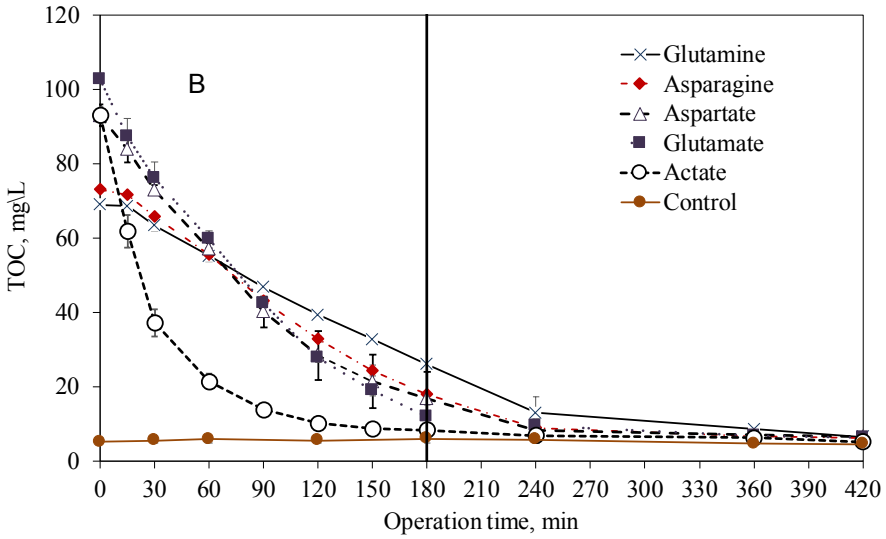
B
Glutamine
Asparagine
Aspartate
Glutamate
Actate
Control
TOC, mg\L
Operation time, min

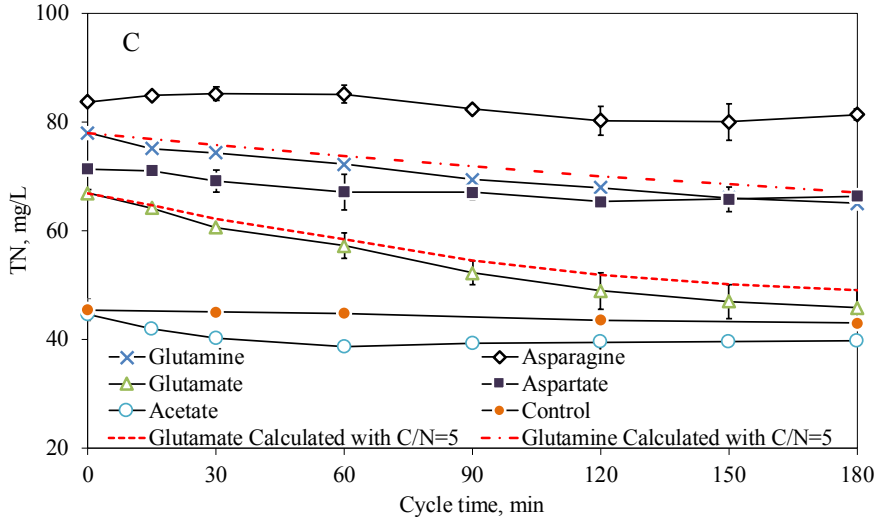
C
Glutamine
Asparagine
Glutamate
Aspartate
Acetate
Control
Glutamate Calculated with C/N=5
Glutamine Calculated with C/N=5
TN, mg/L
Cycle time, min

Figure S6 (**A**) Phosphorous and (**B**) carbon profiles with different amino acids performed in batch reactors operated in parallel and (**C**) the TN profiles during the anaerobic phase (MLSS = 1.6 mg/L; aerobic phase started at 180 min; error bars indicate the range of duplicates).

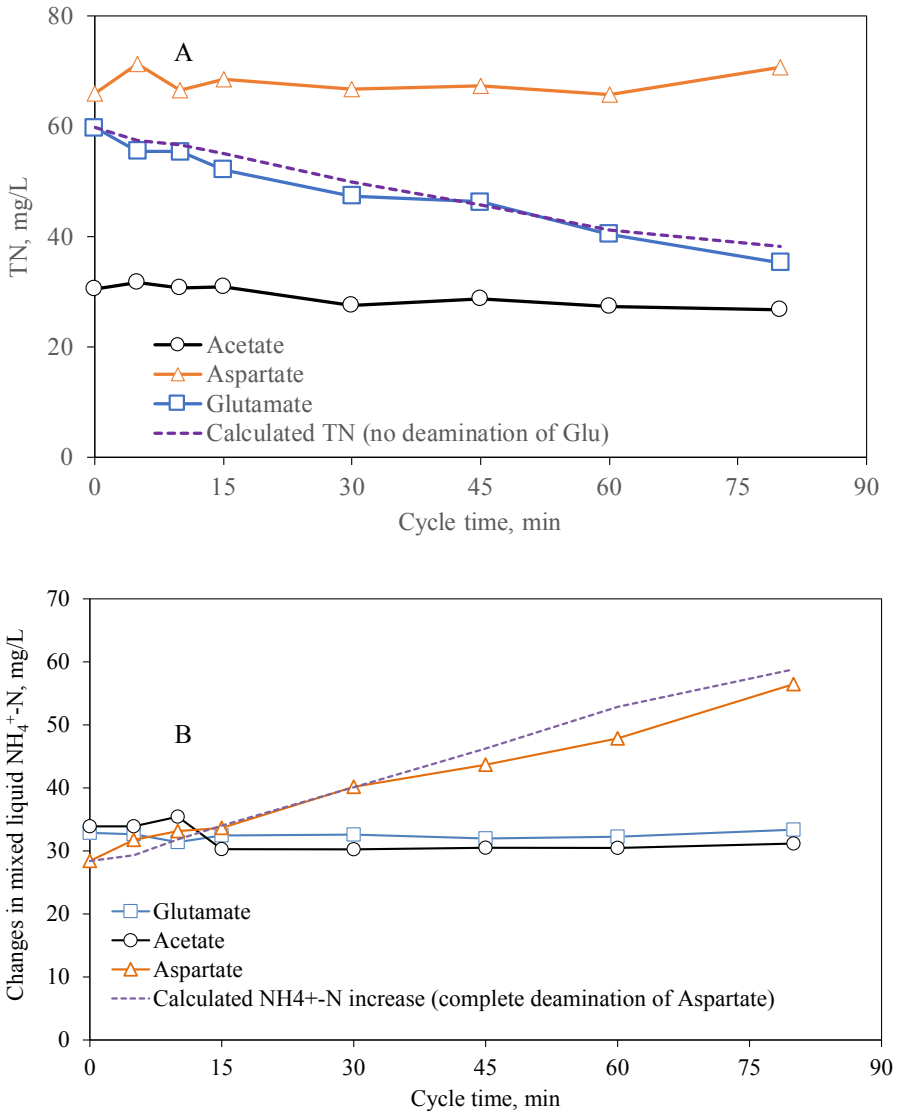

Figure S7 TN (**A**) and NH_4^+-N (**B**) profiles in the cycle study with acetate, aspartate and glutamate as carbon sources.

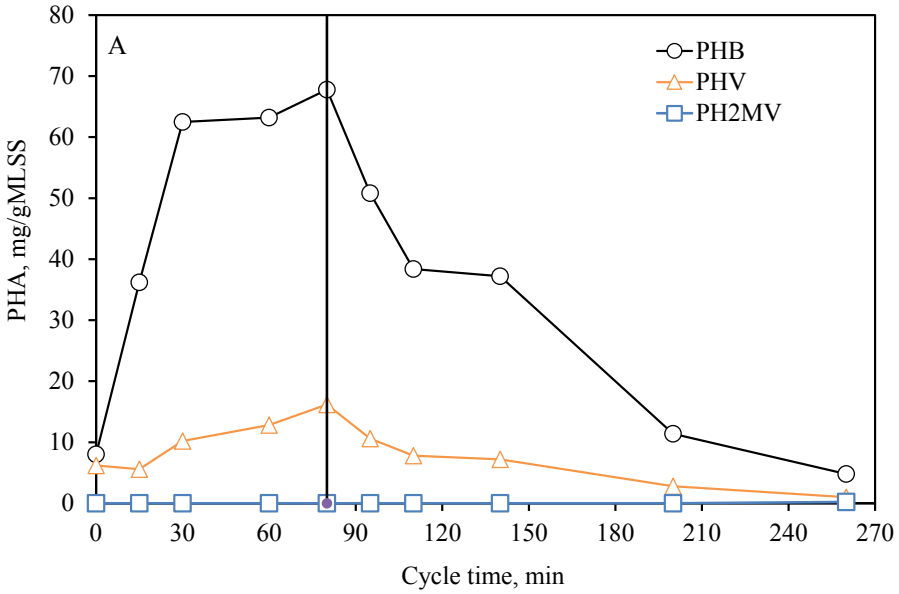
A
PHB
PHV
PH2MV
PHA, mg/gMLSS
Cycle time, min
0
10
20
30
40
50
60
70
80
0
30
60
90
120
150
180
210
240
270

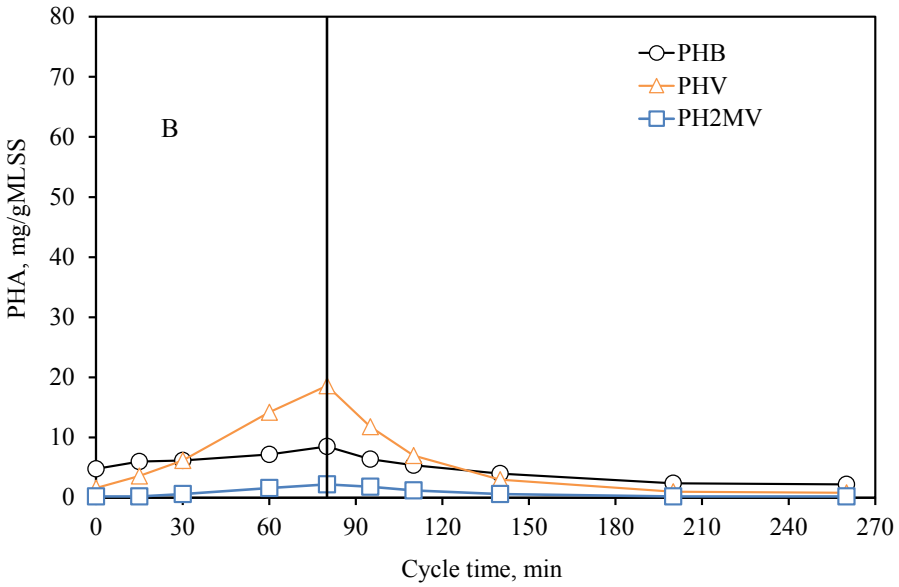
B
PHB
PHV
PH2MV
PHA, mg/gMLSS
Cycle time, min
0
10
20
30
40
50
60
70
80
0
30
60
90
120
150
180
210
240
270

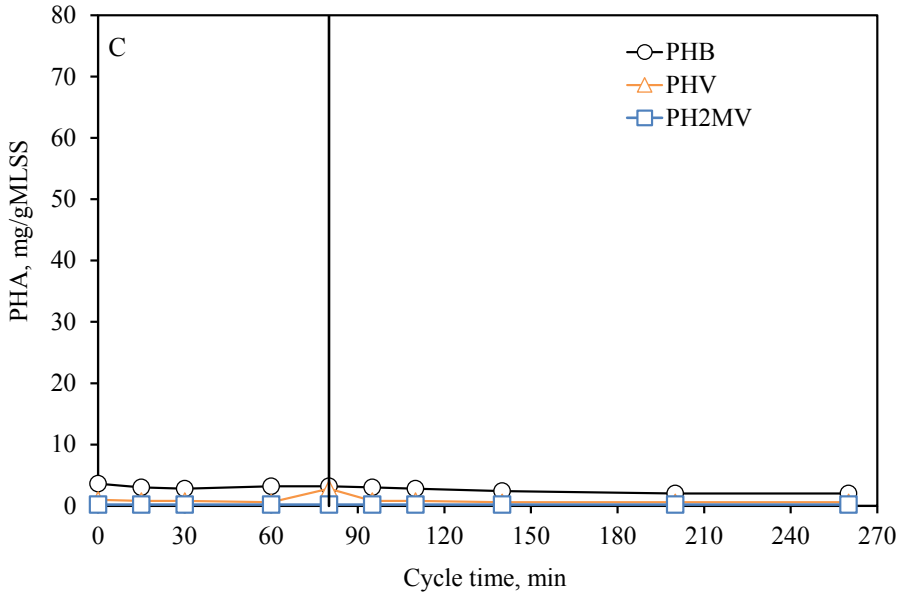

Figure S8 PHA profiles in the cycle study with acetate (**A**), aspartate (**B**) or glutamate (**C**) as a carbon source.

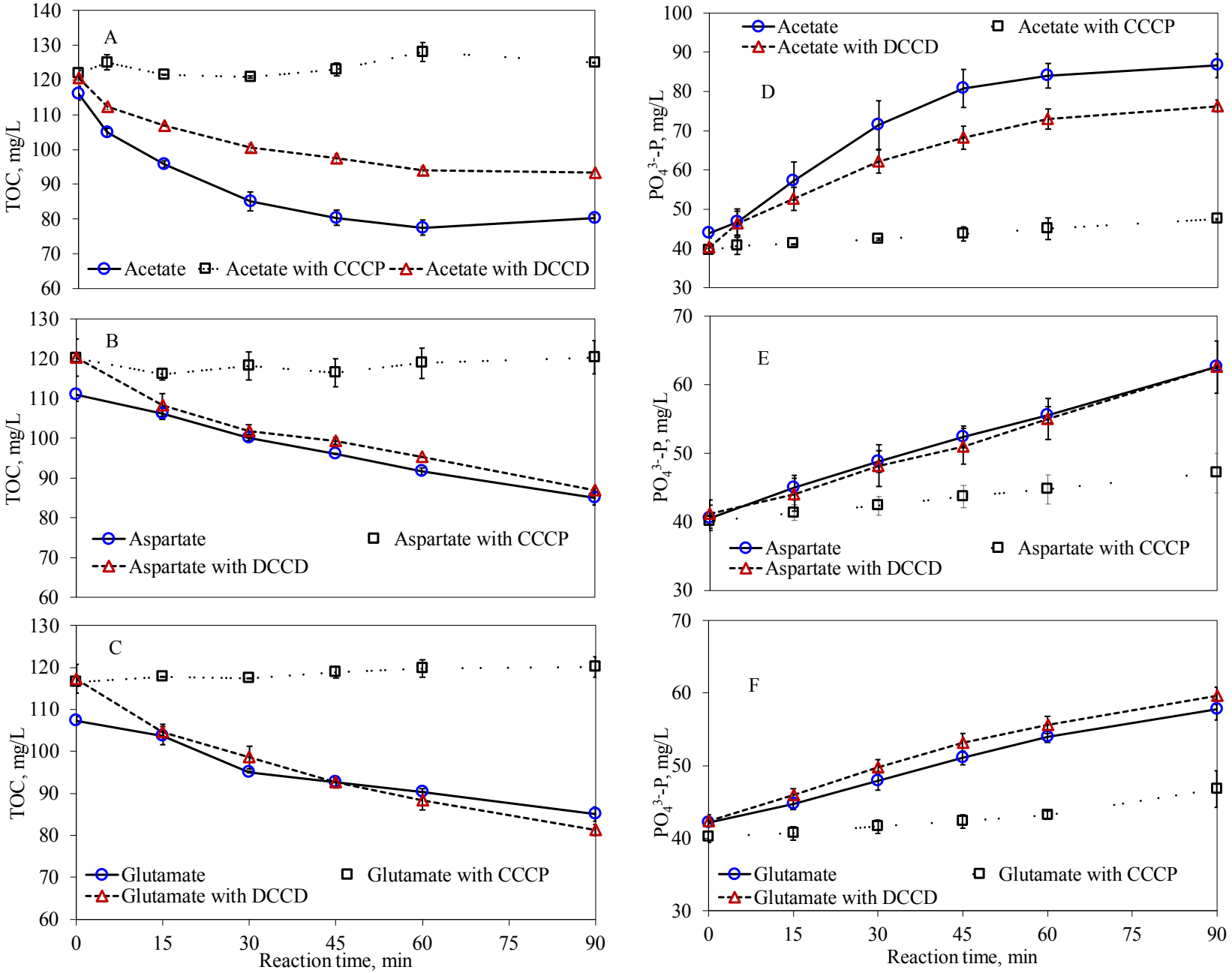
A
TOC, mg/L
Acetate
Acetate with CCCP
Acetate with DCCD
B
Aspartate
Aspartate with CCCP
Aspartate with DCCD
C
Glutamate
Glutamate with CCCP
Glutamate with DCCD
Reaction time, min
D
PO_4^{3-}-P, mg/L
E
F

Figure S9 Anaerobic P release and carbon uptake by *Ca.* Accumulibacter strain SCELSE-1 enrichment culture with and without the PMF decoupler CCCP or the F1-F0 ATPase inhibitor DCCD. (**A**) Carbon (C) uptake for acetate; (**B**) Phosphorus (P) release for acetate; (**C**) C uptake for aspartate; **(D)** P release for aspartate; (**E**) C uptake for glutamate; (**F**) P release for glutamate. Error bars indicate the range of duplicate experiments.

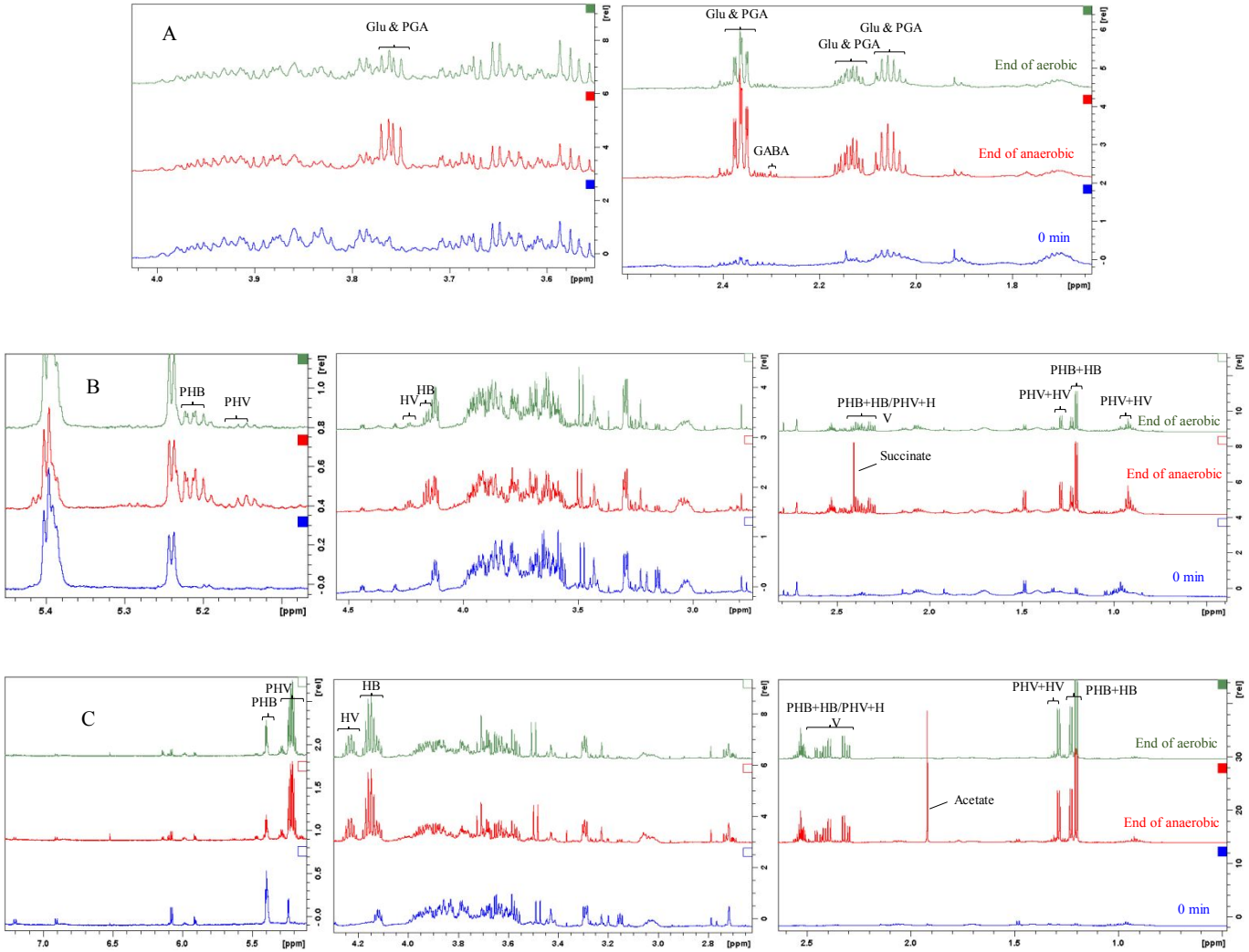

Figure S10 NMR analysis of the intercellular storage compounds when glutamate (**A**), aspartate (**B**) or acetate (**C**) was used as a carbon source.

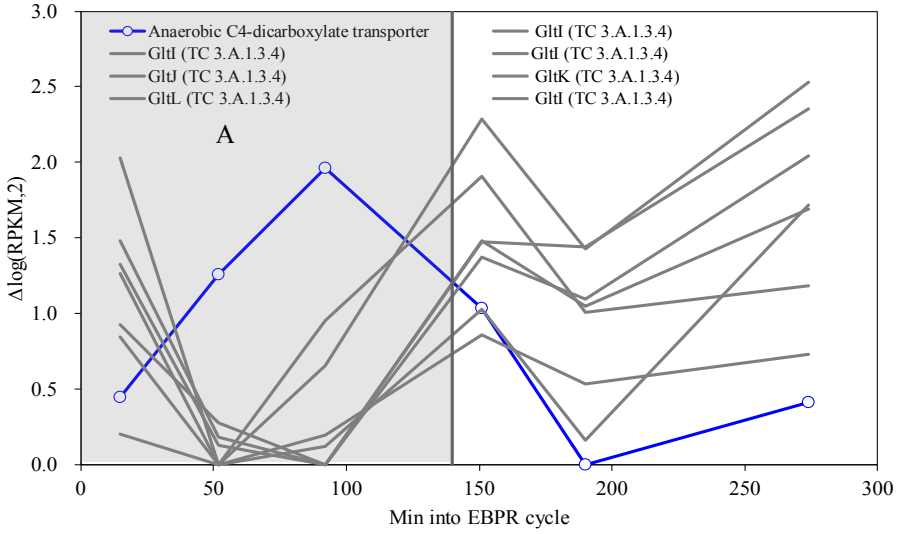
Anaerobic C4-dicarboxylate transporter
GltI (TC 3.A.1.3.4)
GltJ (TC 3.A.1.3.4)
GltL (TC 3.A.1.3.4)
GltI (TC 3.A.1.3.4)
GltI (TC 3.A.1.3.4)
GltK (TC 3.A.1.3.4)
GltI (TC 3.A.1.3.4)
A
Δlog(RPKM,2)
Min into EBPR cycle

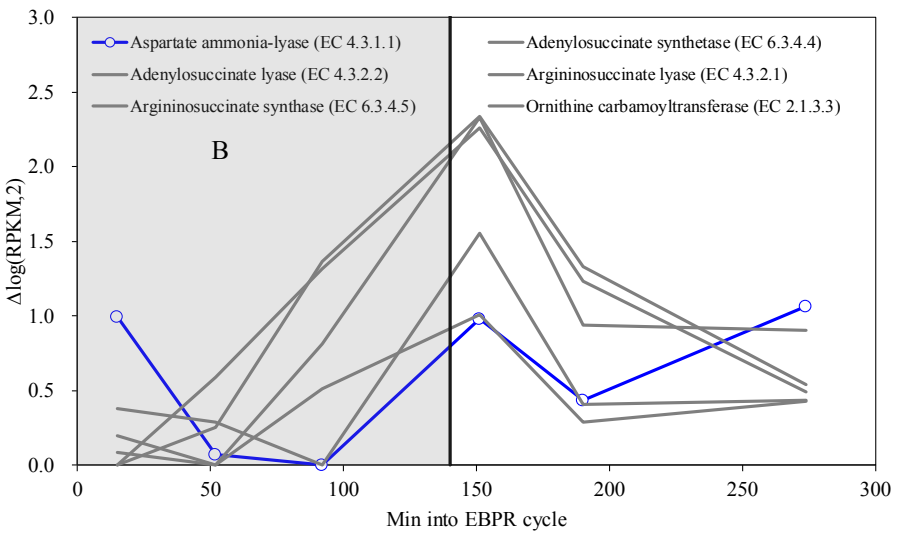
Aspartate ammonia-lyase (EC 4.3.1.1)
Adenylosuccinate lyase (EC 4.3.2.2)
Argininosuccinate synthase (EC 6.3.4.5)
Adenylosuccinate synthetase (EC 6.3.4.4)
Argininosuccinate lyase (EC 4.3.2.1)
Ornithine carbamoyltransferase (EC 2.1.3.3)
B
Δlog(RPKM,2)
Min into EBPR cycle

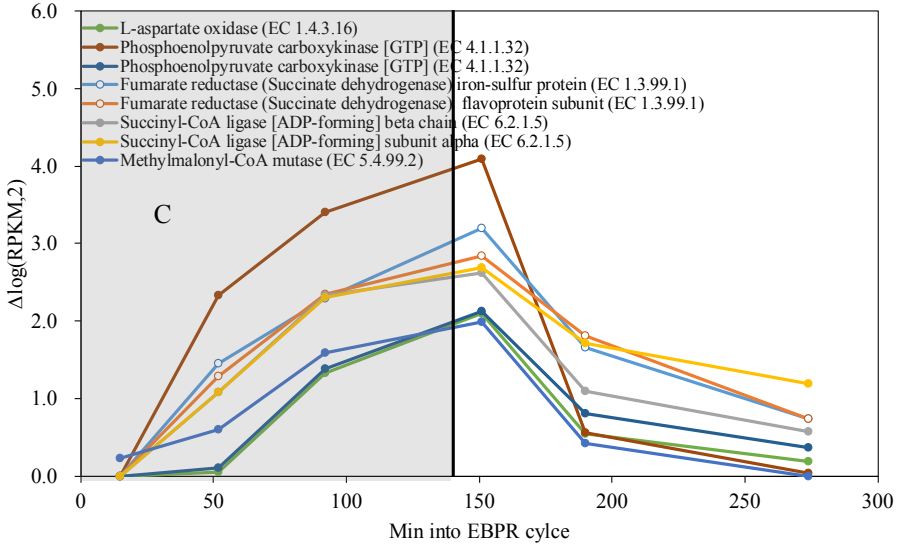
L-aspartate oxidase (EC 1.4.3.16)
Phosphoenolpyruvate carboxykinase [GTP] (EC 4.1.1.32)
Phosphoenolpyruvate carboxykinase [GTP] (EC 4.1.1.32)
Fumarate reductase (Succinate dehydrogenase) iron-sulfur protein (EC 1.3.99.1)
Fumarate reductase (Succinate dehydrogenase) flavoprotein subunit (EC 1.3.99.1)
Succinyl-CoA ligase [ADP-forming] beta chain (EC 6.2.1.5)
Succinyl-CoA ligase [ADP-forming] subunit alpha (EC 6.2.1.5)
Methylmalonyl-CoA mutase (EC 5.4.99.2)
C
Δlog(RPKM,2)
Min into EBPR cylce

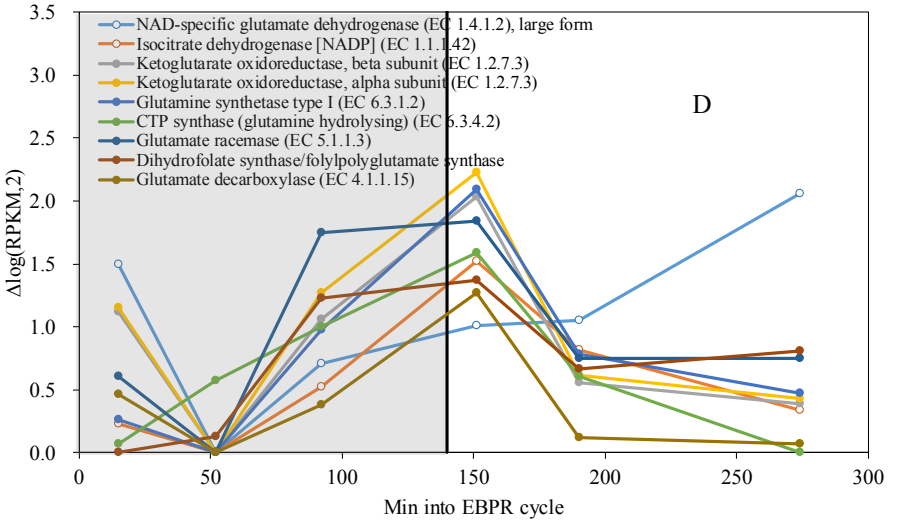
NAD-specific glutamate dehydrogenase (EC 1.4.1.2), large form
Isocitrate dehydrogenase [NADP] (EC 1.1.1.42)
Ketoglutarate oxidoreductase, beta subunit (EC 1.2.7.3)
Ketoglutarate oxidoreductase, alpha subunit (EC 1.2.7.3)
Glutamine synthetase type I (EC 6.3.1.2)
CTP synthase (glutamine hydrolysing) (EC 6.3.4.2)
Glutamate racemase (EC 5.1.1.3)
Dihydrofolate synthase/folylpolyglutamate synthase
Glutamate decarboxylase (EC 4.1.1.15)
D
Δlog(RPKM,2)
Min into EBPR cycle

Figure S11 Gene expression profile patterns (changes in relative transcript abundances were measured as Δlog (RPKM,2), i.e., the difference between the log (RPKM,2) value at each time point and the minimum log (RPKM,2) value in the EBPR cycles for each gene) of the *Ca.* Accumulibacter clade IIA strain UW-1 in a single EBPR cycle. Data were obtained from Oyserman et al., 2016 [34]. Yeast extract was included in the feed when the authors performed the metatranscriptomic analysis. The expression patterns of genes related to aspartate and glutamate metabolism of *Ca.* Accumulibacter clade IIA stain UW-1 may provide evidences to support the proposed pathways in this work. Gray and white backgrounds represent anerobic and aerobic phases respectively. **A**. The expression of a homologue gene (CAP2UW1_1862) of *glt*P encoding a C4-dicarboxylate transport protein increased anaerobically and decreased aerobically. While genes encoding the glutamate/aspartate transport system (*glt*I, *glt*K, *glt*J and *glt*L, K1001–K1004),[14] belonging to the ATP-binding cassette (ABC) transporter family showed decreased expressions after anaerobic carbon contact. Their expressions were relatively high under aerobic condition. These results are in line with the observations in this work where the uptake of aspartate and glutamate were achieved via GltP driven by PMF and were not via the glutamate/aspartate ABC transporter. **B**. Expression patterns of genes involved in the fumarate generation from aspartate. Genes involved in purine nucleotide cycle (EC: 6.3.4.4; EC: 4.3.2.2) and urea cycle (EC: 6.3.4.5; EC: 4.3.2.1) was expressed increasingly in the anaerobic phase and decreasingly in the aerobic phase. No specific pattern was observed for a gene encoding the aspartate ammonia-lyase (EC: 4.3.1.1). These results implied that both purine nucleotide cycle and urea cycle might have been active for the conversion of aspartate to fumarate in *Ca.* Accumulibacter clade IIA stain UW-1. While where was probably no significant direct conversion of aspartate to fumarate via aspartate ammonia-lyase. **C**. Expression of key genes involved in the aspartate metabolic pathway proposed in this study increased anaerobically and decreased after exposure to oxygen. They include genes encoding L-aspartate oxidase (EC 1.4.3.16, responsible for the conversion of aspartate to oxaloacetate), phosphoenolpyruvate carboxykinase

(EC 4.1.1.32, oxaloacetate to phosphoenolpyruvate), fumarate reductase (EC 1.3.5.1, EC 1.3.5.4, fumarate to succinate), and succinyl-CoA ligase (EC 6.2.1.5, succinate activation to succinyl-CoA), methylmalonyl-CoA mutase (EC 5.4.99.2, succinyl-CoA to methylmalonyl-CoA). **D.** Expression patterns of key genes involved in the glutamine/glutamate metabolic pathway (and the metabolic pathway with the co-presence of acetate and glutamate) proposed in this work. The gene encoding the glutamate dehydrogenase (EC 1.4.1.2) more highly expressed in the aerobic phase than in the anaerobic phase, which is in line with the observation that a majority of glutamate was not deaminized or routed to the TCA cycle, but was stored in a different form during the anaerobic phase. The high expression of genes encoding the glutamate racemase (EC 5.1.1.3) and folylpolyglutamate (FPGA) synthase (EC 6.3.2.17) during the anaerobic phase also supports the hypothesis that glutamate was stored as glutamate polymers (FPGA/PGA). The high anaerobic expression of isocitrate dehydrogenase (EC 1.1.1.42) and ketoglutarate oxidoreductase (EC 1.2.7.3) was probably related to the use of the TCA cycle to generate reducing power [37] by *Ca.* Accumulibacter clade IIA stain UW-1 or the activation of the glutamate/acetate pathway proposed in this work, or both.

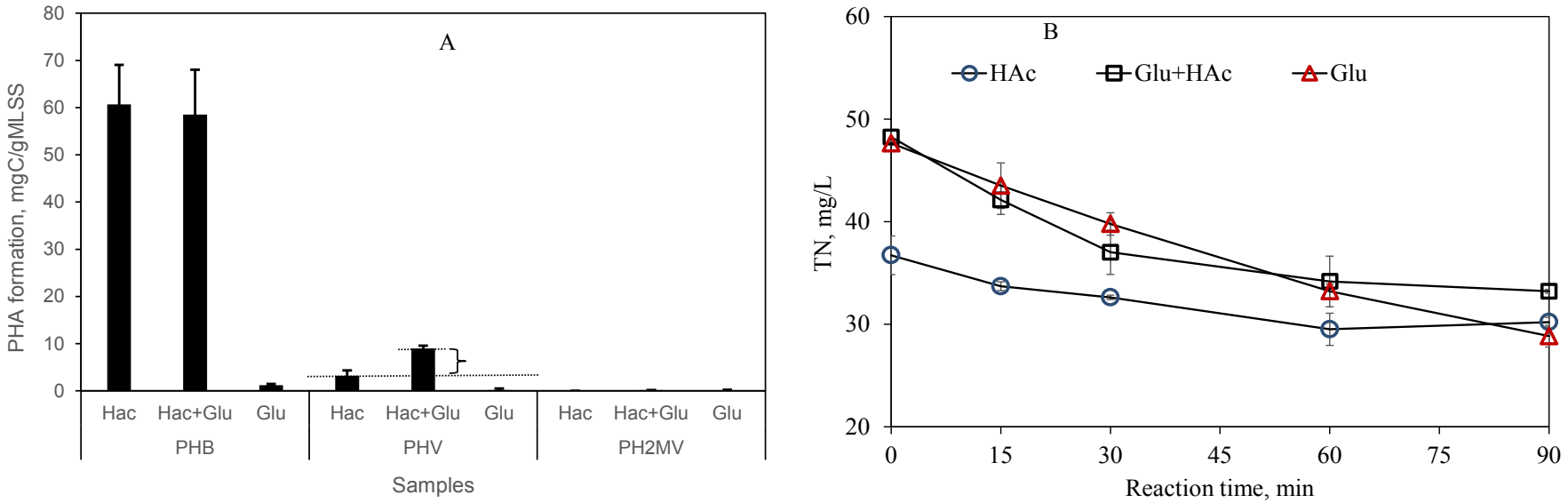

Figure S12 (**A**) PHA formation characteristics and TN (**B**) profiles with the co-presence of glutamate (Glu) and acetate (HAc) as compared to these with acetate or glutamate as a single carbon source. Error bars indicate the range of duplicate experiments.

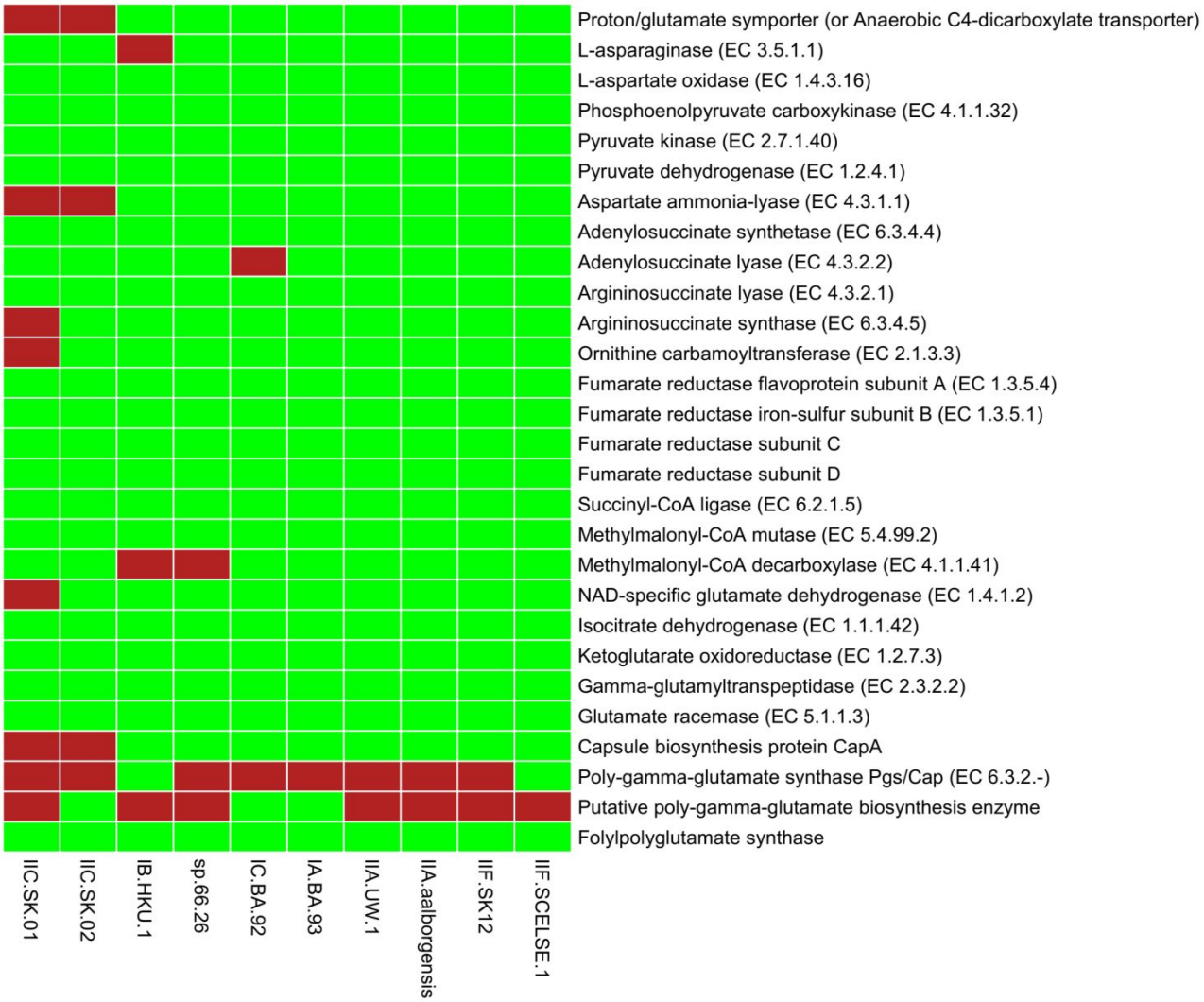

Figure S13 Presence (Green) and absence (Red) of key genes involved in the metabolism of aspartate and glutamate in draft genomes of representative *Ca.* Accumulibacter stains.

References

(1) Albertsen, M.; Karst, S.M.; Ziegler, A.S.; Kirkegaard, R.H.; Nielsen, P.H. Back to basics–the influence of DNA extraction and primer choice on phylogenetic analysis in activated sludge communities. *PLoS ONE* **2015**, 10: e0132783.

(2) McIlroy, S. J.; Saunders, A. M.; Albertsen, M.; Nierychlo, M.; McIlroy, B.; Hansen, A.A.; Karst, S.M.; Nielsen, J.L.; Nielsen P.H. MiDAS: the field guide to the microbes of activated sludge. *Database* **2015**, 1–8.

(3) Bolger, A.M.; Lohse, M.; Usadel, B., Trimmomatic: A flexible trimmer for Illumina Sequence Data. *Bioinformatics* **2014**, 30(15), 2114–2120.

(4) Peng, Y.; Leung, H.C.M.; Yiu S.M., Chin F.Y.L., IDBA-UD: a de novo assembler for single-cell and metagenomic sequencing data with highly uneven depth. *Bioinformatics* **2012**, 28, 1420–1428.

(5) Langmead, B.; Salzberg, S. Fast gapped-read alignment with Bowtie 2. Nat. Methods **2012**, 9, 357–359.

(6) Li, H.; Handsaker, B.; Wysoker, A.; Fennell, T.; Ruan, J.; Homer, N.; Marth, G.; Abecasis, G.; Durbin, R. and 1000 Genome Project Data Processing Subgroup. The Sequence alignment/map (SAM) format and SAMtools. *Bioinformatics* **2009**, 25, 2078-2079.

(7) Alneberg, J.; Bjarnason, B.S.; de Bruijn, I.; Schirmer, M.; Quick, J.; Ijaz, U.Z.; Lahti, L.; Loman, N.J.; Andersson A.F.; Quince. C., Binning metagenomic contigs by coverage and composition. *Nat. Methods* **2014**, 11, 1144–1146.

(8) Parks, D.H.; Imelfort, M.; Skennerton, C.T.; Hugenholtz, P.; Tyson, G.W., Assessing the quality of microbial genomes recovered from isolates, single cells, and metagenomes. *Genome Res.*, **2014**, 25, 1043–1055.

(9) Ondov, B.D.; Treangen, T.J.; Melsted, P.; Mallonee, A.B.; Bergman, N.H.; Koren, S.; Phillippy, A.M., Mash: fast genome and metagenome distance estimation using MinHash. *Genome Biol.* **2016**, 17(1), 132: doi: 10.1186/s13059-016- 0997-x.

(10) Gillespie, J.J.; Wattam, A.R.; Cammer, S.A.; Gabbard, J.L.; Shukla, M.P.; Dalay, O.; Driscoll, T.; Hix, D.; Mane, S.P.; Mao, C.; Nordberg, E.K.; Scott, M.; Schulman J.R.; Snyder, E.E.; Sullivan, D.E.; Wang, C.; Warren, A.; Williams, K.P.; Xue. T.; Yoo H.S.; Zhang, C.; Zhang, Y.; Will, R.; Kenyon, R.W.; Sobral, B.W., PATRIC: the comprehensive bacterial bioinformatics resource with a focus on human pathogenic species. *Infect Immun.* **2011**, 79(11), 4286–4298.

(11) Goris, J.; Konstantinidis, K.T.; Klappenbach, J.A.; Coenye, T.; Vandamme, P.; Tiedje, J.M. DNA-DNA hybridization values and their relationship to whole-genome sequence similarities. *Int. J. Syst. Evol. Micr.* **2007**, 57, 81-91.

(12) Richter, M.; Rosselló-Móra, R. Shifting the genomic gold standard for the prokaryotic species definition. *Proc. Natl. Acad. Sci. USA*, **2009**, 106, 19126-19131.

(13) Gurevich, A.; Saveliev, V.; Vyahhi N.; Tesler, G., QUAST: quality assessment tool for genome assemblies. *Bioinformatics*, **2013**, 29(8), 1072–1075.

(14) Seemann, T., Prokka: rapid prokaryotic genome annotation. Bioinformatics. 2014, 30(14), 2068–2069.

(15) Miller, C.S.; Baker, B.J.; Thomas, B.C.; Singer, S.W.; Banfield, J.F., 2011, EMIRGE: reconstruction of full-length ribosomal genes from microbial community short read sequencing data. *Genome Biol.* 12, R44: doi:10.1186/gb-2011-12-5-r44.

(16) Pruesse, E.; Peplies, J.; Glöckner, F.O., SINA: accurate high-throughput multiple sequence alignment of ribosomal RNA genes. *Bioinformatics* **2012**, 28, 1823–1829.

(17) Camejo, P.Y., Oyserman, B.O.; McMahon, K.D.; Noguera, D.R., 2019. Integrated omic analyses provide evidence that a "*Candidatus* Accumulibacter phosphatis" strain performs denitrification under microaerobic conditions. *mSystems* **4**, e00193-18: doi.org/10 .1128/mSystems.00193-18.

(18) Mao, Y.; Yu, K.; Xia, Y.; Chao, Y.; Zhang T., Genome reconstruction and gene expression of "*Candidatus* Accumulibacter phosphatis" clade IB performing biological phosphorus removal. *Environ. Sci. Technol.* **2014**, 48(17), 10363–10371.

(19) Na, S.I.; Kim, Y.O.; Yoon, S.H.; Ha, S.M.; Baek, I.; Chun, J. UBCG: Up-to-date bacterial core gene set and pipeline for phylogenomic tree reconstruction. J. Microbiol. 2018, 56(4), 280-285.

(20) Daims, H.; Brühl, A.; Amann, R.; Schleifer, K.H.; Wagner, M. The domain-specific probe EUB338 is insufficient for the detection of all bacteria: Development and evaluation of a more comprehensive probe set. *Syst. Appl. Microbiol.* **1999**, 22, 434–444.

(21) Crocetti, G.R.; Hugenholtz, P.; Bond, P.L.; Schuler, A.; Keller, J.; Jenkins, D.; Blackall1, L.L.; Identification of polyphosphate-accumulating organisms and design of 16S rRNA directed probes for their detection and quantitation. *Environ. Microbiol.* **2000**, 66, 1175–1182.

(22) Crocetti, G.R.; Banfield, J.F.; Keller, J.; Bond, P.L.; Blackall, L.L. Glycogen-accumulating organisms in laboratory-scale and full-scale wastewater treatment processes. *Microbiology* **2002**, 148(11), 3353–3364.

(23) Smolders G.J.F.; van der Meij J.; van Loosdrecht M.C.M.; Heijnen J.J. Model of the anaerobic metabolism of the biological phosphorus removal process: stoichiometry and pH influence. *Biotechnol. Bioeng.* **1994**, 43, 461–470.

(24) Saunders A.M.; Mabbett A.N.; McEwan A.G.; Blackall L.L. Proton motive force generation from stored polymers for the uptake of acetate under anaerobic conditions. *FEMS Microbiol. Lett.* **2007**.274, 245–251.

(25) Burow, L.; Mabbett, A.; McEwan, A.; Bond, P.; Blackall, L. Bioenergetic models for acetate and phosphate transport in bacteria important in enhanced biological phosphorus removal. *Environ. Microbiol.* **2008**, 10, 87–98.

(26) Bossi, R.T.; Negri, A.; Tedeschi, G.; Mattevi, A. Structure of FAD-bound L-aspartate oxidase: insight into substrate specificity and catalysis. *J. Biochem.* **2002**, 41, 3018–3024.

(27) Salway, J.G. *Metabolism at a glance 3rd edition*, Blackwell Publishing Ltd., Oxford, 2004.

(28) Harvey, R.A.; Ferrier, D.R. *Lippincott's Illustrated Reviews, Biochemistry, 5th ed.* Lippincott Williams & Wilkins, 2011.

(29) Hilpert, W.; Dimroth P. Conversion of the chemical energy of methylmalonyl-CoA decarboxylation into a Na^+ gradient. *Nature* **1982**, 296, 584-585.

(30) Marques, R.; Santos, J.; Nguyen, H.; Carvalho, G.; Noronha, J.P.; Nielsen, P.H.; Reis, M.A.M.; Oehmen, A. Metabolism and ecological niche of *Tetrasphaera* and *Ca.* Accumulibacter in enhanced biological phosphorus removal. *Water Res.* **2017**, 122, 159–171.

(31) Zengin, G.E.; Artan, N.; Orhon, D.; Satoh, H.; Mino, T. Effect of aspartate and glutamate on the fate of enhanced biological phosphorus removal process and microbial community structure. *Bioresour. Technol*. **2011**, 102(2), 894–903.

(32) Camacho, M.L.; Brown, R.A.; Bonete, M.J.; Danson M.J.; Hough, D.W. Isocitrate dehydrogenases from *Haloferax volcanii* and *Sulfolobus solfataricus*: enzyme purification, characterisation and N-terminal sequence. *FEMS Microbiol. Lett.* **1995**. 134, 85–90.

(33) Nguyen, H.T.T.; Kristiansen, R.; Vestergaard, M.; Wimmer, R.; Nielsen, P.H. Intracellular accumulation of glycine in polyphosphate-accumulating organisms in activated sludge, a novel storage mechanism under dynamic anaerobic-aerobic conditions. *Appl. Environ. Microbiol.* **2015**, 81(14), 4809-4818.

(34) Oyserman, B.O.; Noguera, D.R.; del Rio, T.G.; Tringe, S.G.; McMahon K.D. Metatranscriptomic insights on gene expression and regulatory controls in Candidatus Accumulibacter phosphatis. ISME J. 2016, 10, 810–822.

(35) Kumar, S.; Stecher, G.; Tamura, K., MEGA7: Molecular evolutionary genetics analysis version 7.0 for bigger datasets. *Mol. Biol. Evol.* 2016, **33**, 1870–1874.

(36) Nielsen, J.L.; Kragelund, C.; Nielsen, P.H. Combination of fluorescence in situ hybridization with staining techniques for cell viability and accumulation of PHA and polyP in microorganisms in complex microbial systems. In: Cummings, S. (Ed.). *Methods in Molecular Biology. Bioremediation*. Humana Press Inc. **2010**, 599, 103-116.

(37) Zhou, Y.; Pijuan, M.; Zeng, R.J.; Yuan, Z. Involvement of the TCA cycle in the anaerobic metabolism of polyphosphate accumulating organisms (PAOs). *Water Res*. **2009**, 43, 1330–1340.